



*Supplement of*

## **Comprehensive Global Assessment of 24 Gridded Precipitation Datasets Across 18 428 Catchments Using Hydrological Modeling**

**Ather Abbas et al.**

*Correspondence to:* Hylke E. Beck ([hylke.beck@kaust.edu.sa](mailto:hylke.beck@kaust.edu.sa))

The copyright of individual parts of the supplement might differ from the article licence.

## Supplementary Contents

<b>S1 Performance Comparison Across Köppen-Geiger Climate Zones</b>	<b>2</b>
<b>S2 Spatial Maps of Calibration Performance for <math>P</math> Datasets</b>	<b>4</b>
<b>S3 Performance Variation Across Streamflow Data Sources</b>	<b>28</b>
<b>S4 Impact of Rain Gauge Density on Model Performance</b>	<b>30</b>
<b>S5 Scenario Analysis of Calibration Strategies</b>	<b>31</b>
<b>S6 Differences in Mean Annual Precipitation</b>	<b>35</b>
<b>S7 Performance Variation with Altitude</b>	<b>48</b>

# S1 Performance Comparison Across Köppen-Geiger Climate Zones

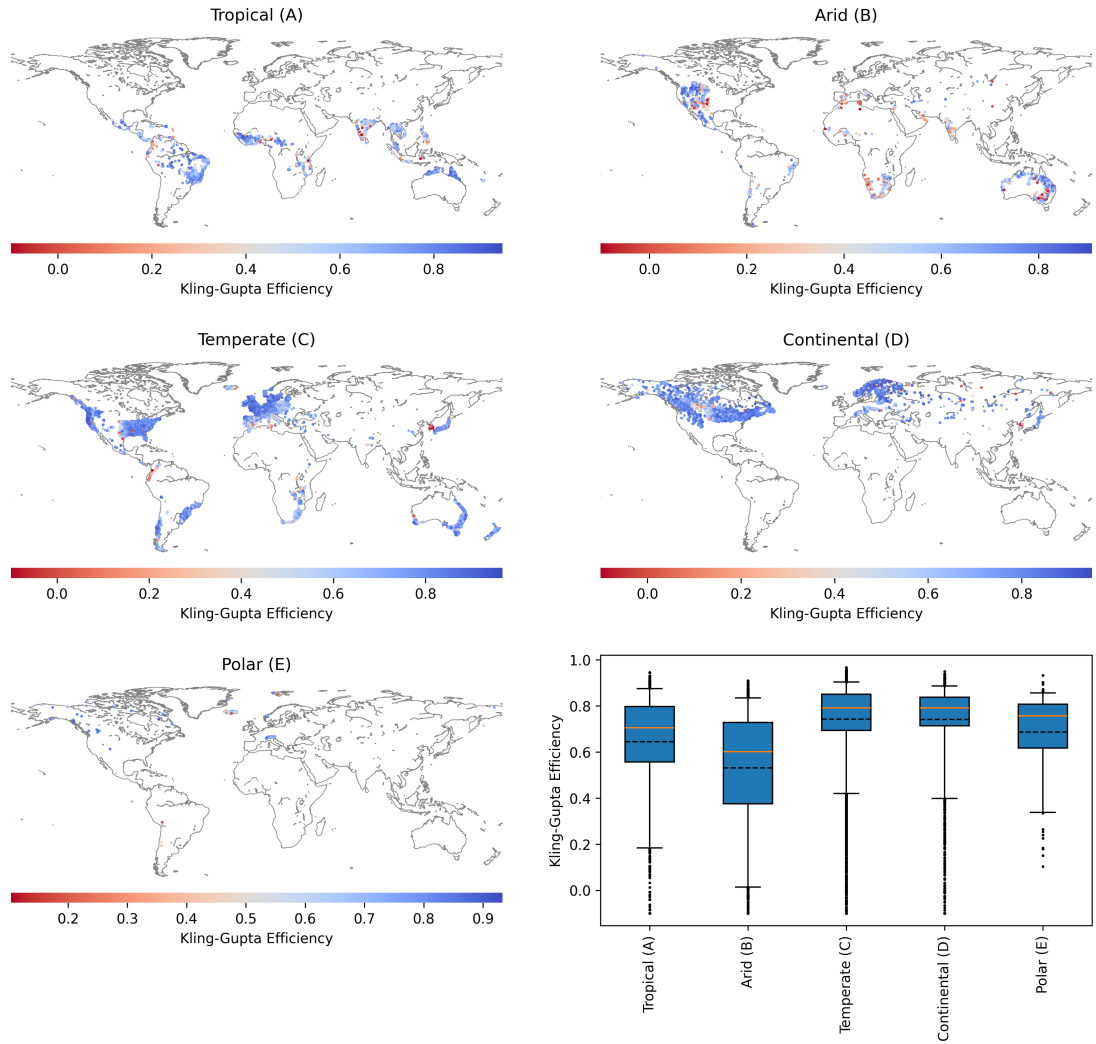


Figure S1: Spatial maps and distribution of Kling-Gupta Efficiency for MSWEP V2.8 dataset.

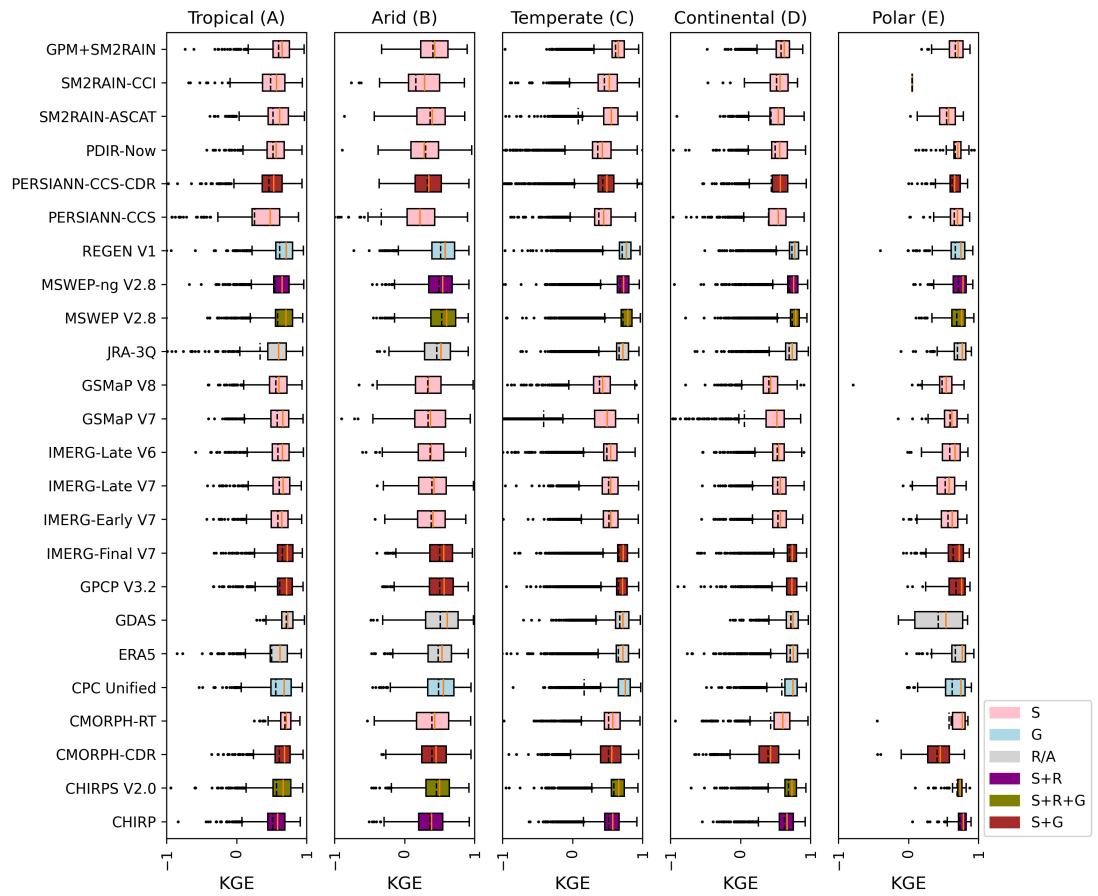


Figure S2: Performance of 24 P datasets in major Köppen-Geiger climate zones.

## S2 Spatial Maps of Calibration Performance for $P$ Datasets

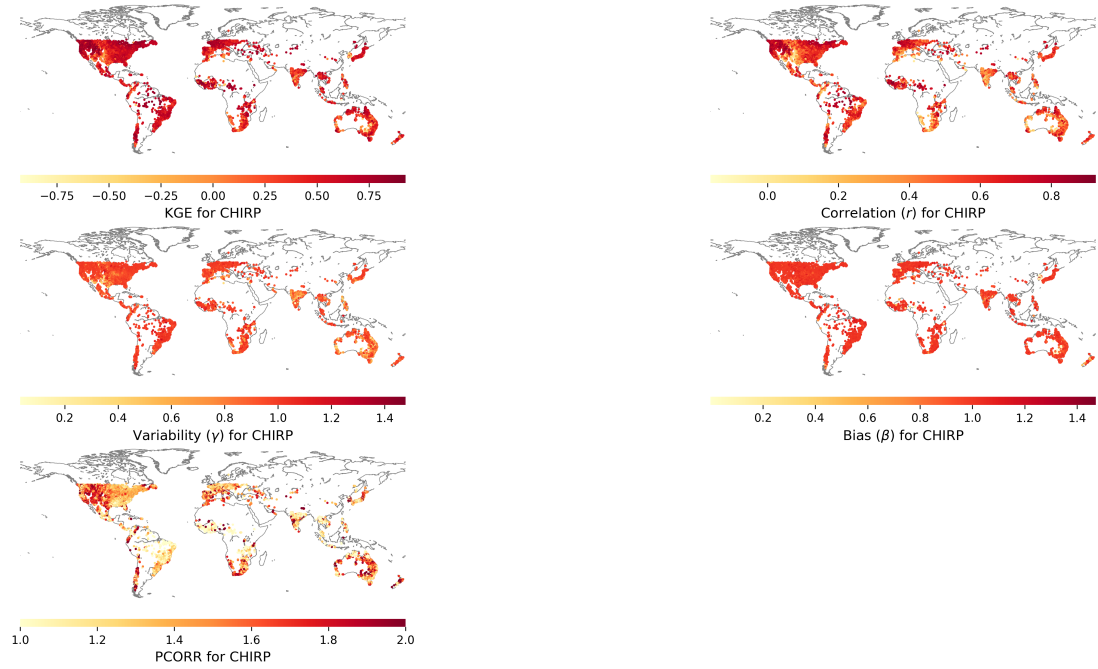


Figure S3: Calibration performance (KGE, correlation, variability, and bias) and PCORR values for CHIRP.

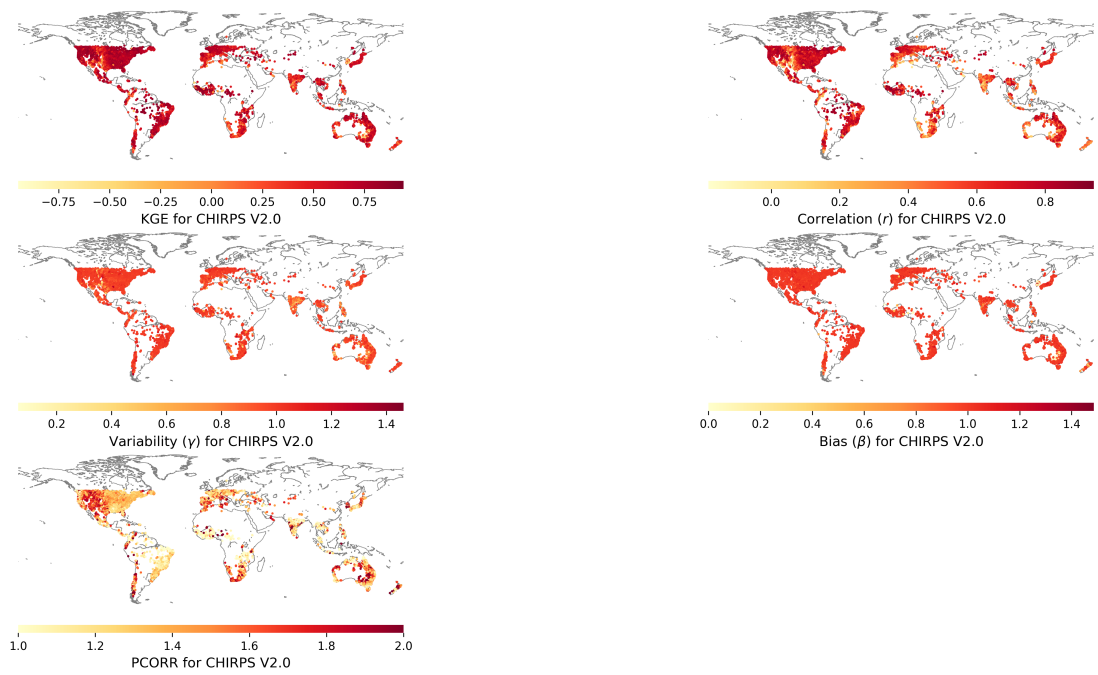


Figure S4: Calibration performance (KGE, correlation, variability, and bias) and PCORR values for CHIRPS V2.0.

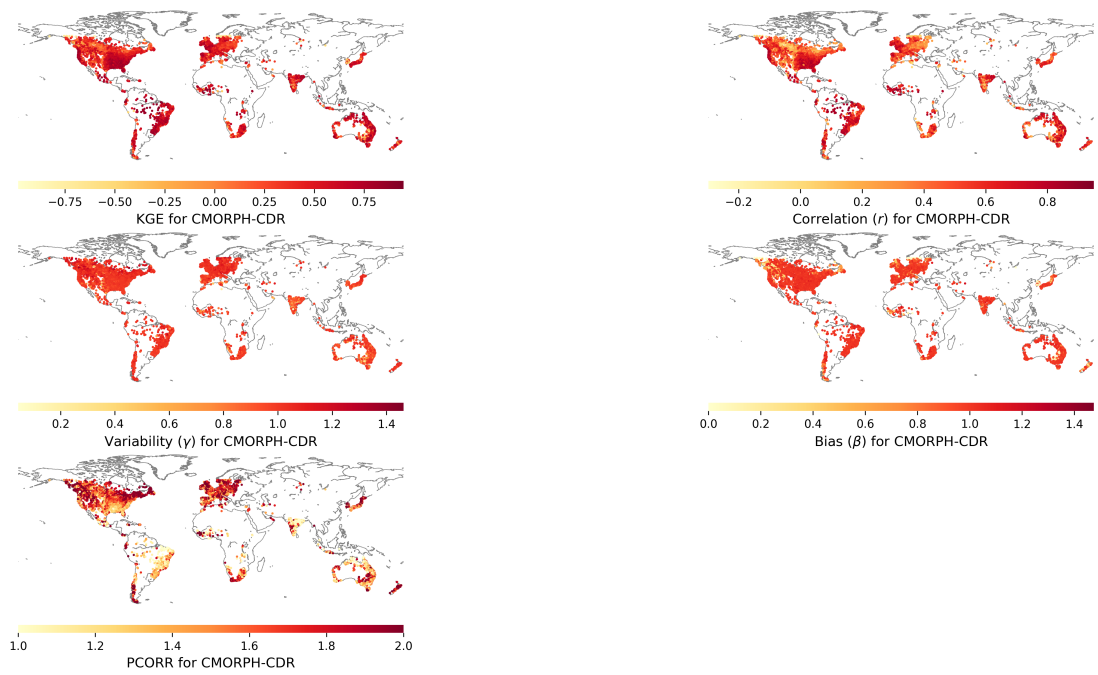


Figure S5: Calibration performance (KGE, correlation, variability, and bias) and PCORR values for CMORPH-CDR.

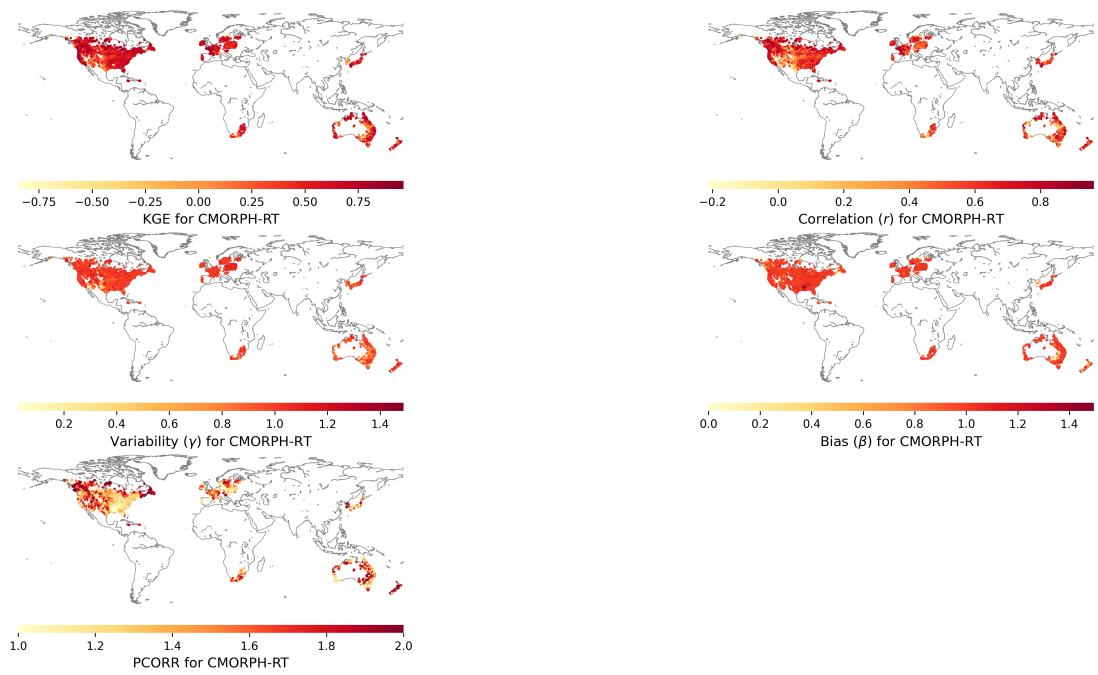


Figure S6: Calibration performance (KGE, correlation, variability, and bias) and PCORR values for CMORPH-RT.

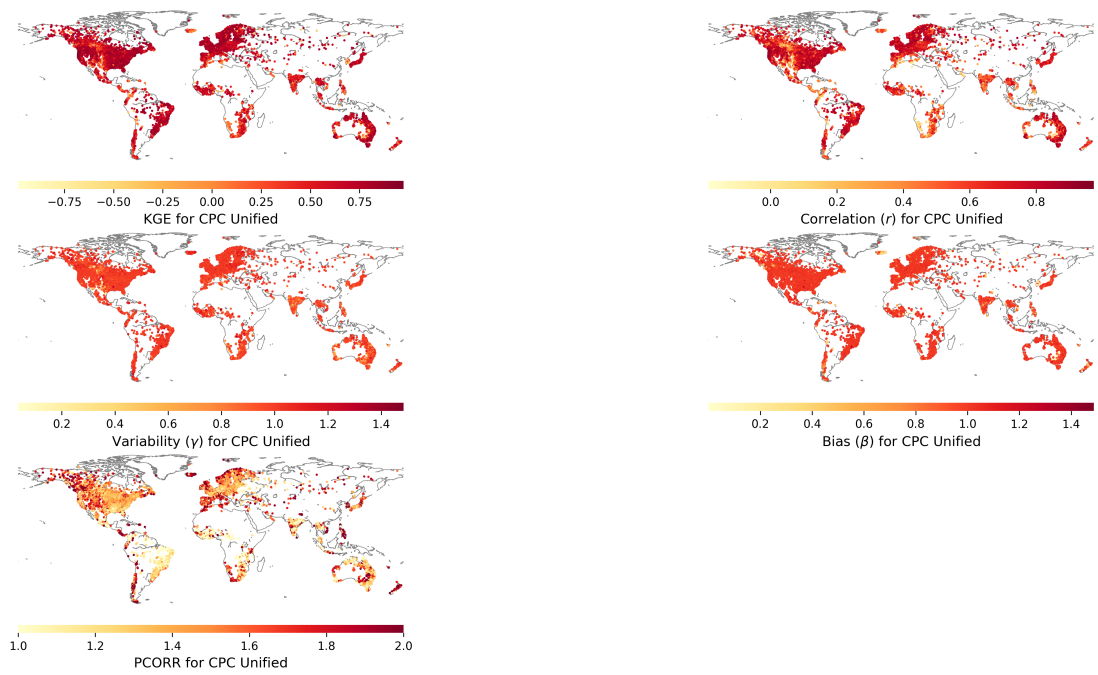


Figure S7: Calibration performance (KGE, correlation, variability, and bias) and PCORR values for CPC Unified.

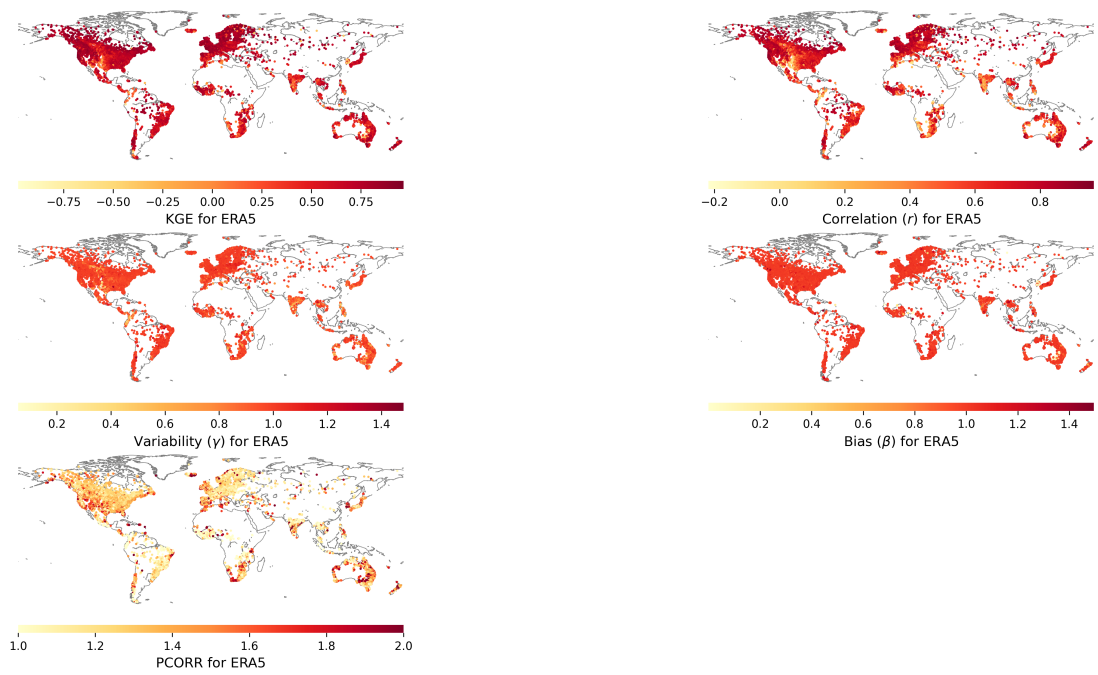


Figure S8: Calibration performance (KGE, correlation, variability, and bias) and PCORR values for ERA5.

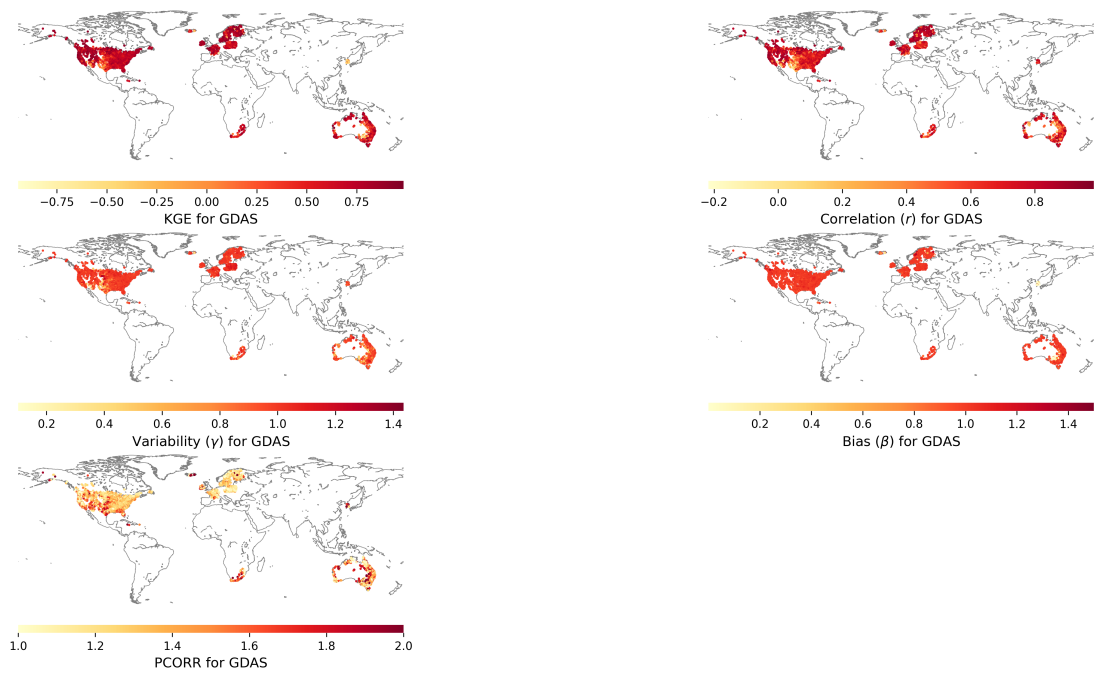


Figure S9: Calibration performance (KGE, correlation, variability, and bias) and PCORR values for GDAS.

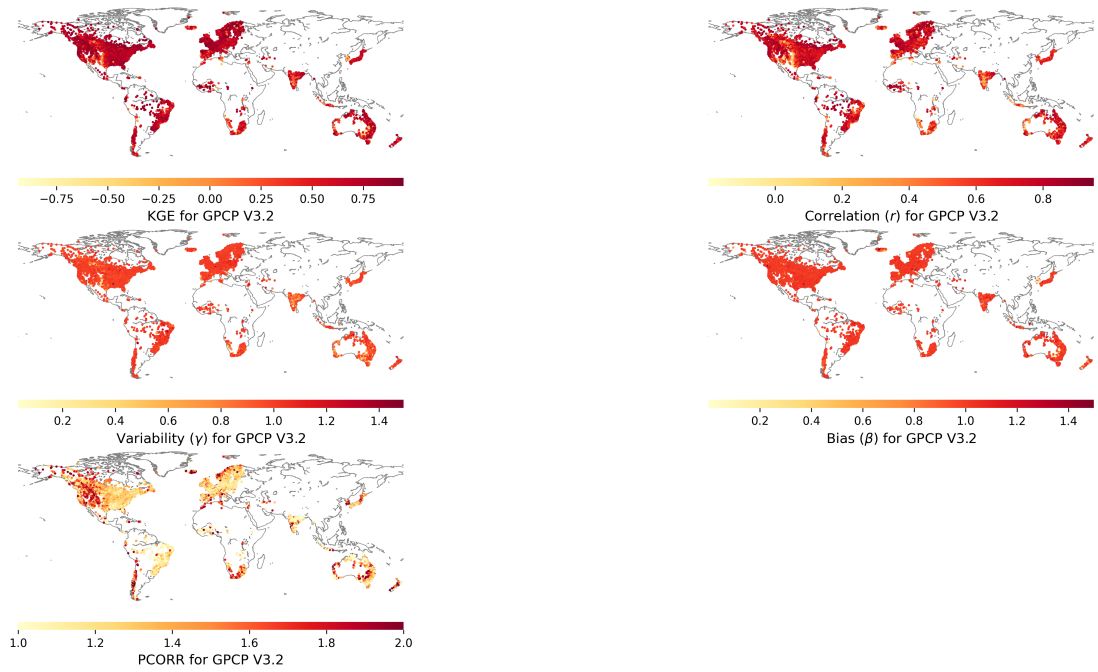


Figure S10: Calibration performance (KGE, correlation, variability, and bias) and PCORR values for GPCP V3.2.

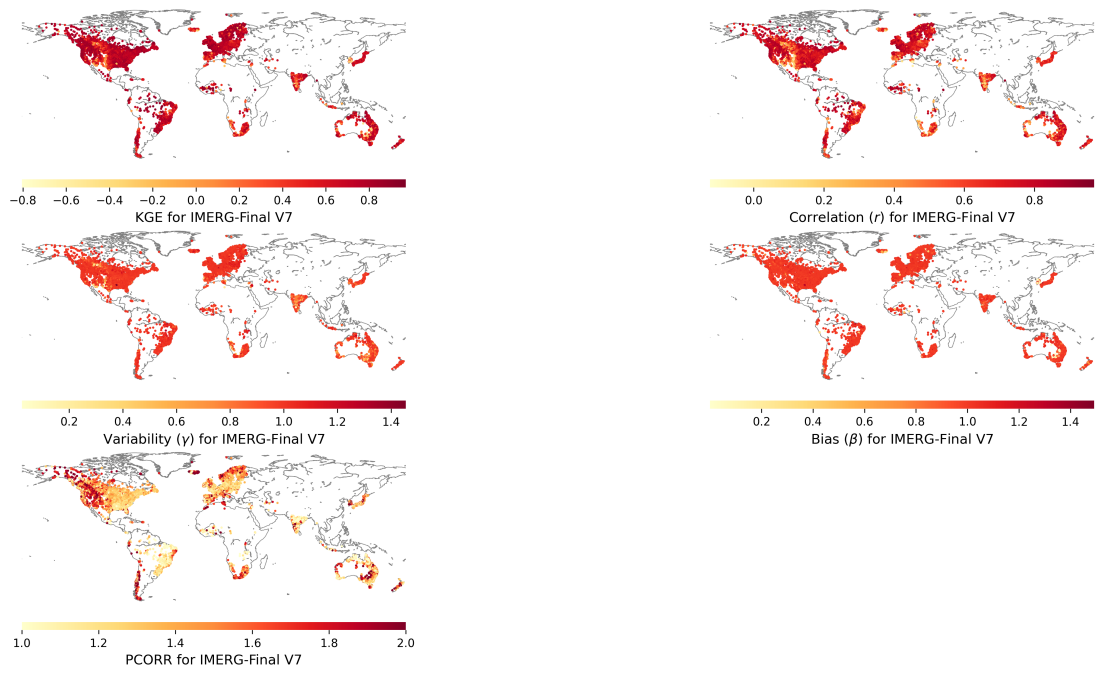


Figure S11: Calibration performance (KGE, correlation, variability, and bias) and PCORR values IMERG-Final V7.

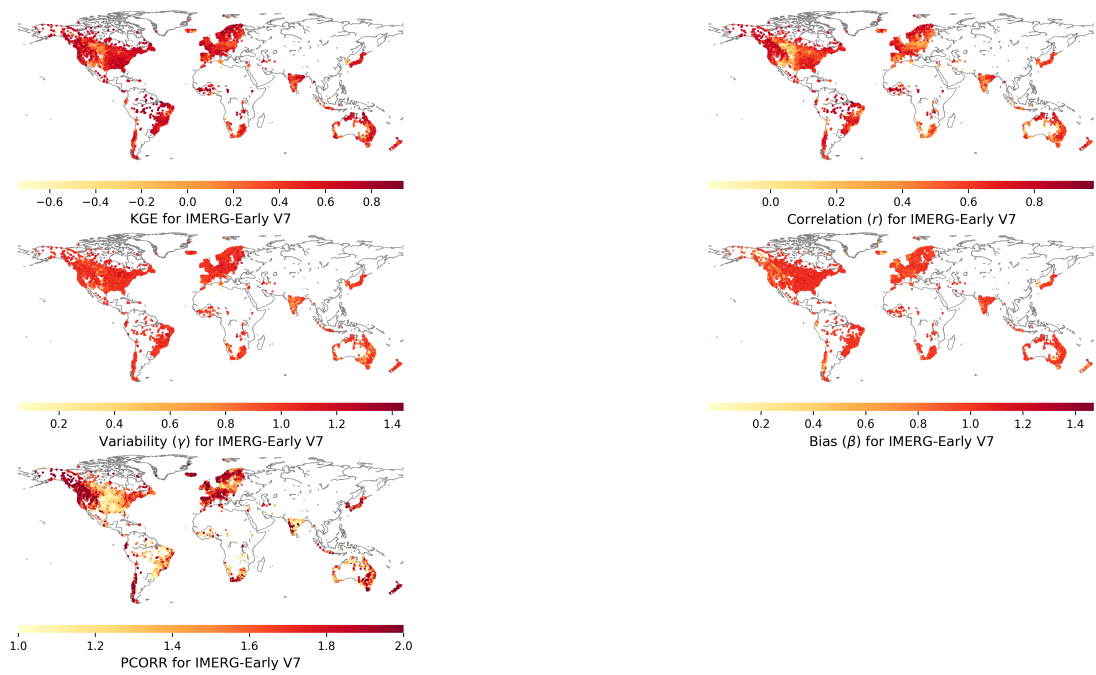


Figure S12: Calibration performance (KGE, correlation, variability, and bias) and PCORR values for IMERG-Early V7.

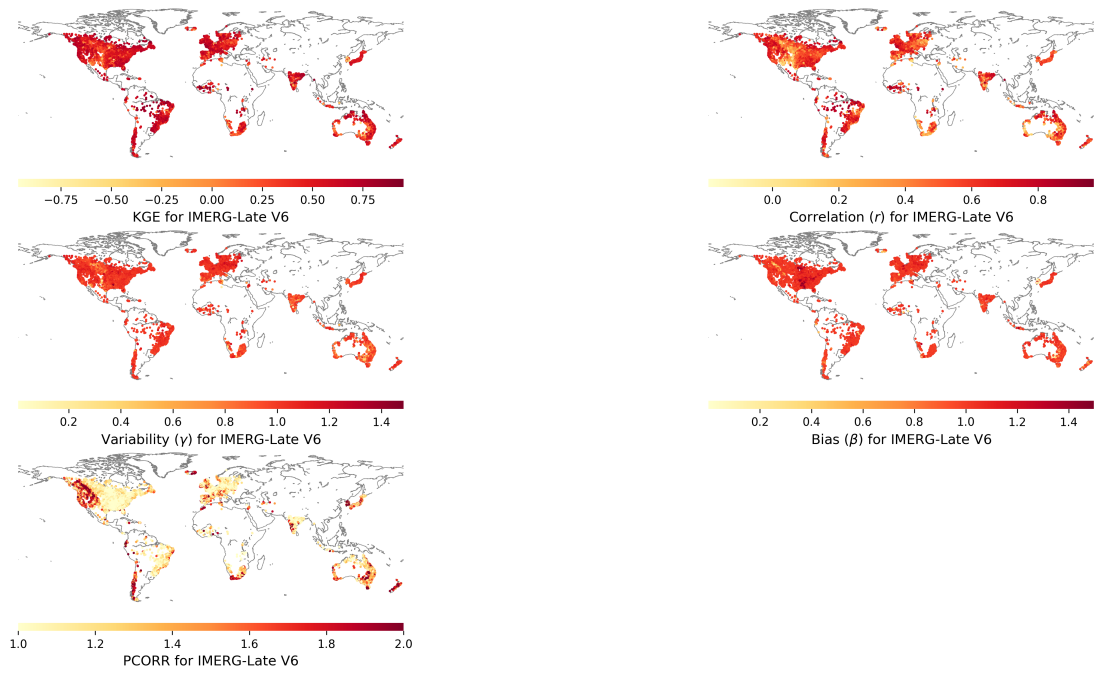


Figure S13: Calibration performance (KGE, correlation, variability, and bias) and PCORR values for IMERG-Late V6.

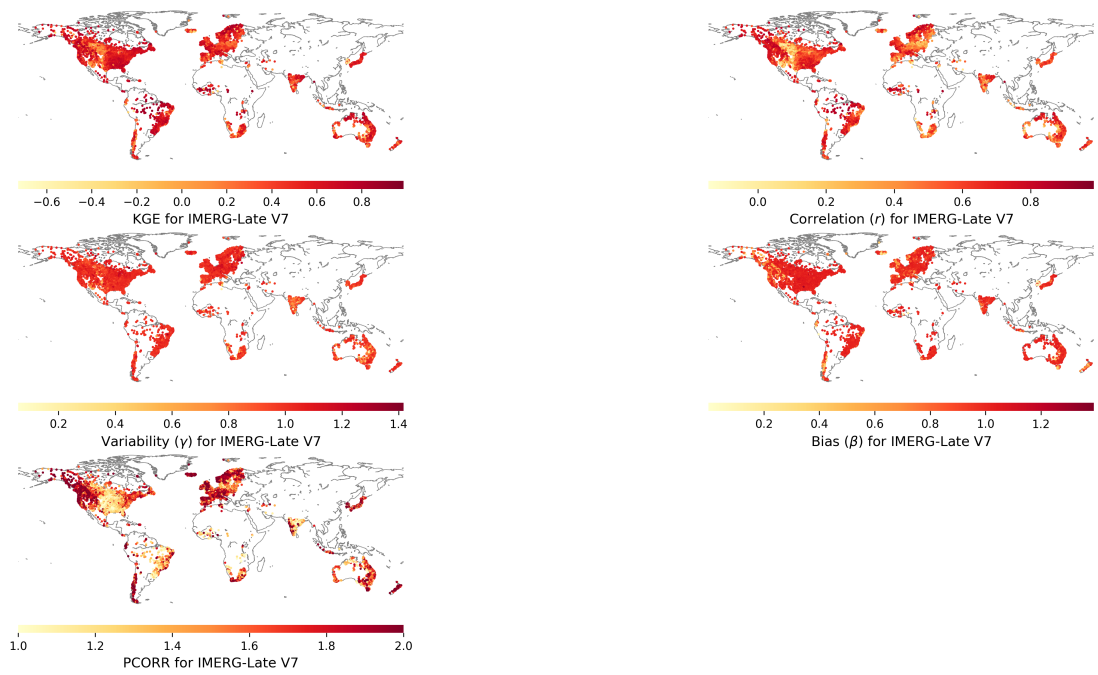


Figure S14: Calibration performance (KGE, correlation, variability, and bias) and PCORR values for IMERG-Late V7.

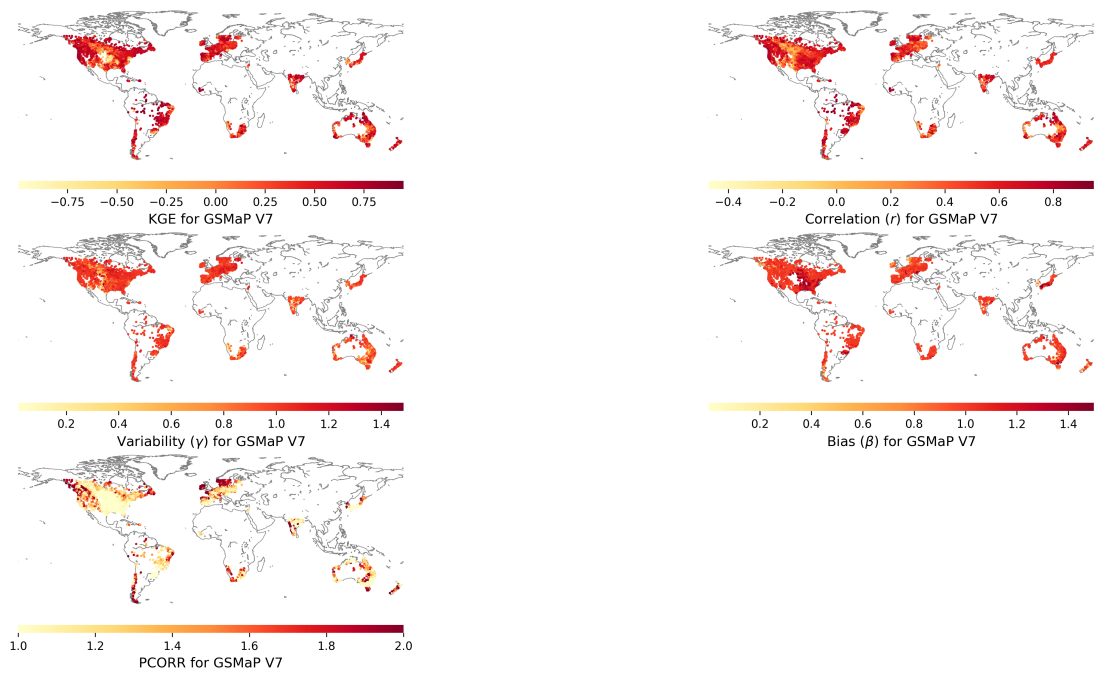


Figure S15: Calibration performance (KGE, correlation, variability, and bias) and PCORR values achieved for GSMaP V7.

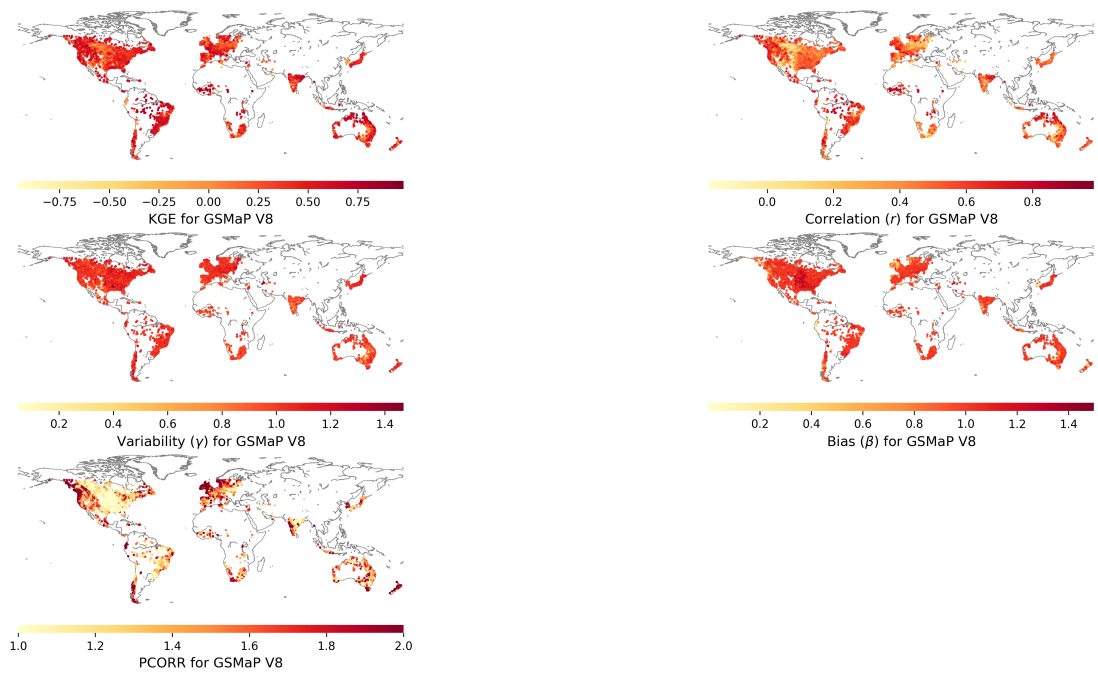


Figure S16: Calibration performance (KGE, correlation, variability, and bias) and PCORR values for GSMaP V8.

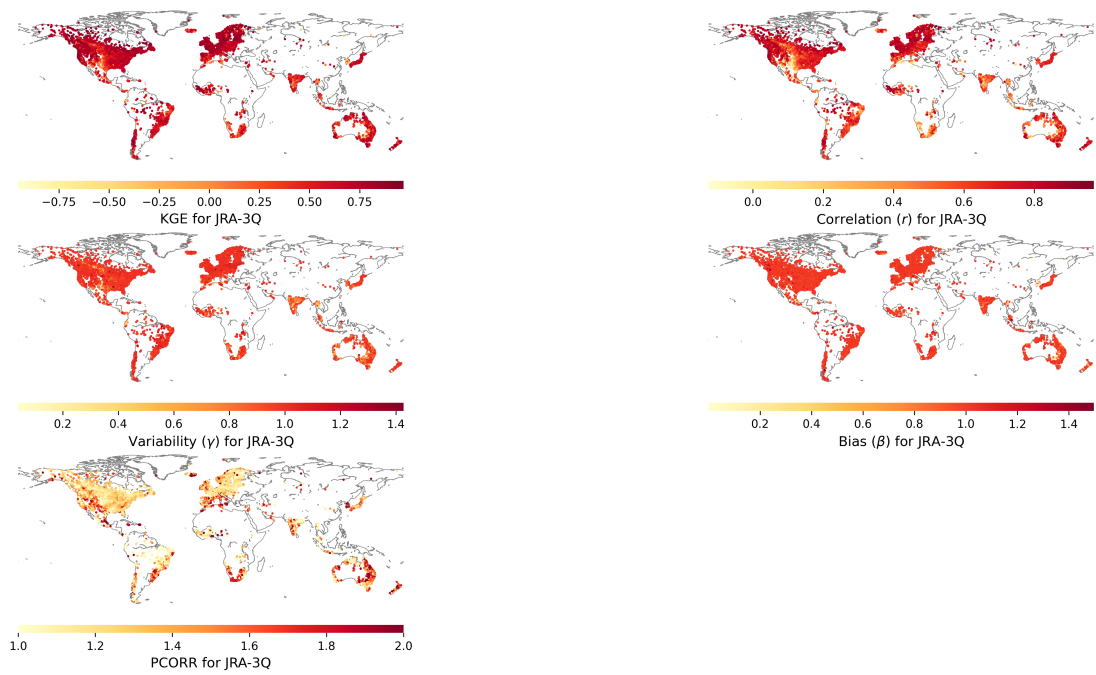


Figure S17: Calibration performance (KGE, correlation, variability, and bias) and PCORR values for JRA-3Q.

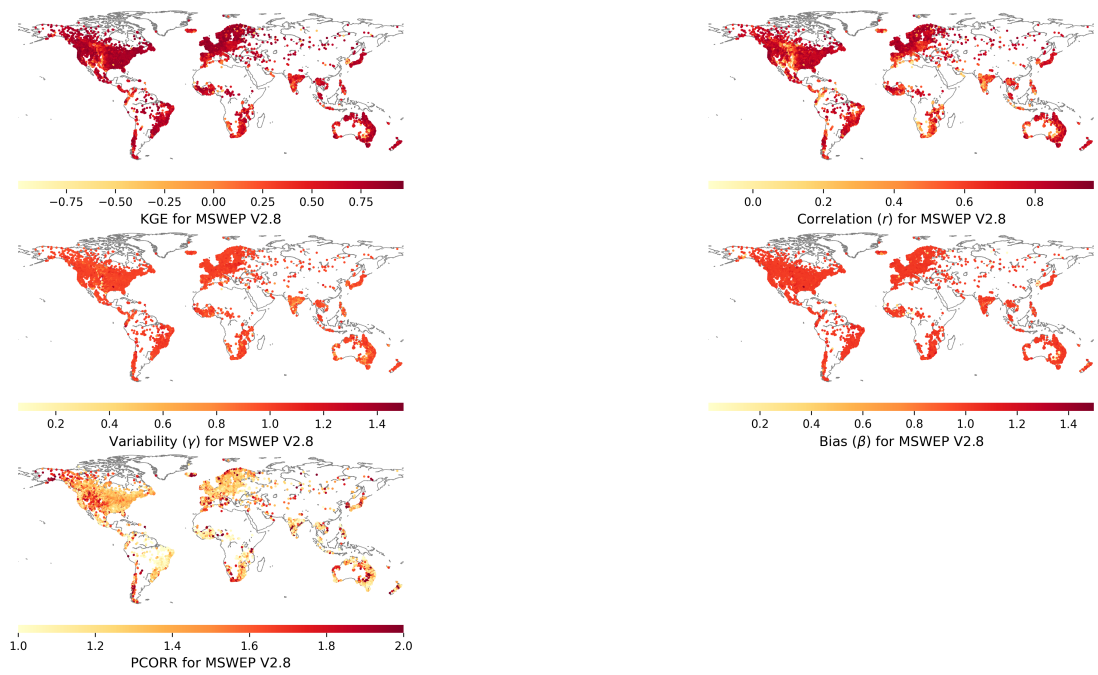


Figure S18: Calibration performance (KGE, correlation, variability, and bias) and PCORR values for MSWEP V2.8.

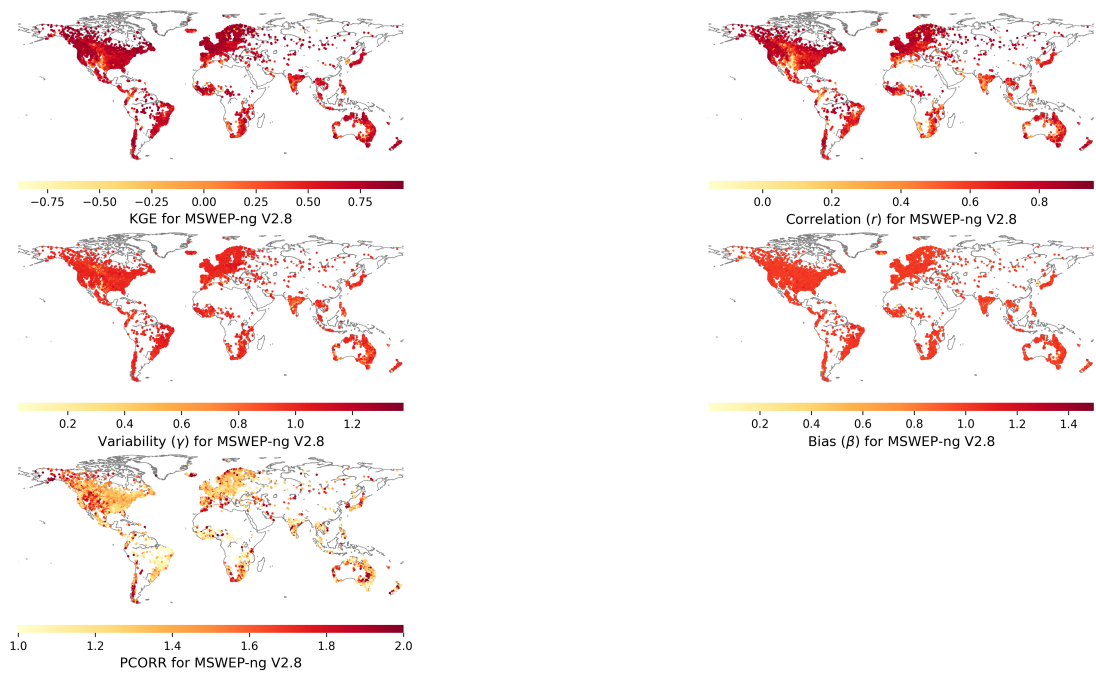


Figure S19: Calibration performance (KGE, correlation, variability, and bias) and PCORR values for MSWEP-ng V2.8 dataset.

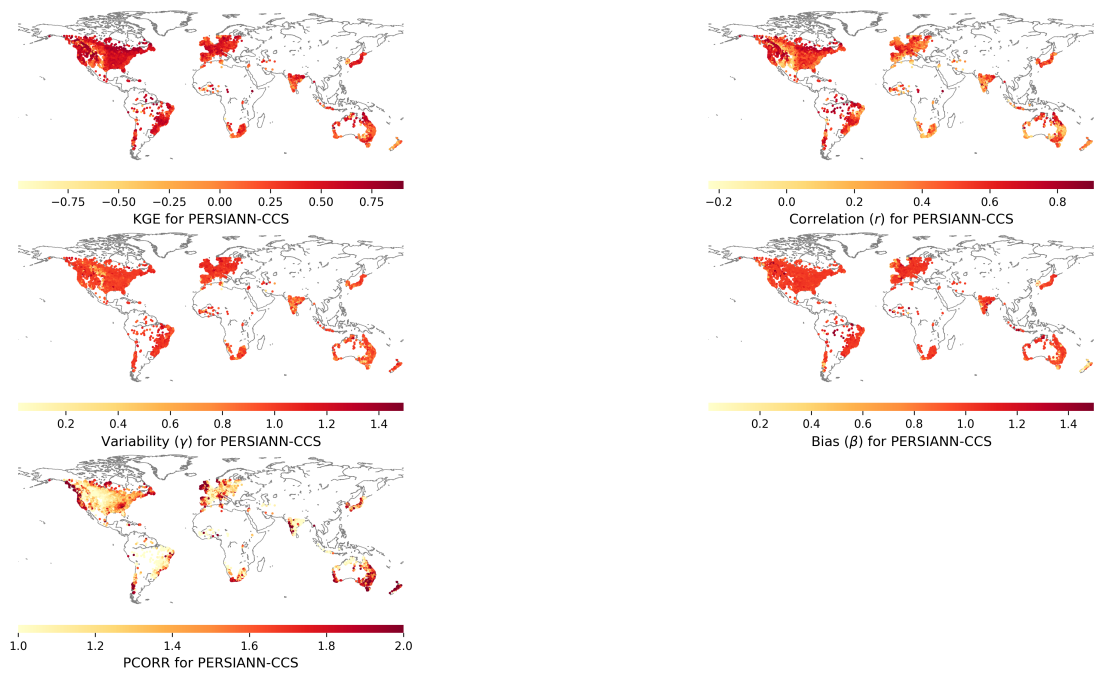


Figure S20: Calibration performance (KGE, correlation, variability, and bias) and PCORR values for PERSIANN-CCS.

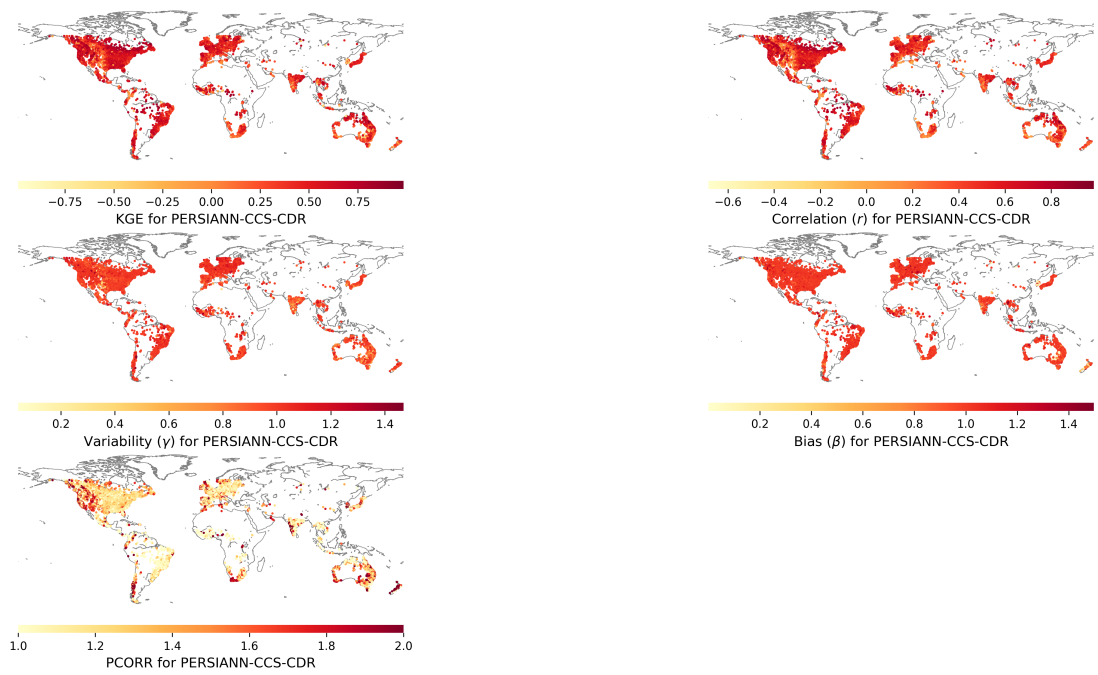


Figure S21: Calibration performance (KGE, correlation, variability, and bias) and PCORR values for PERSIANN-CCS-CDS.

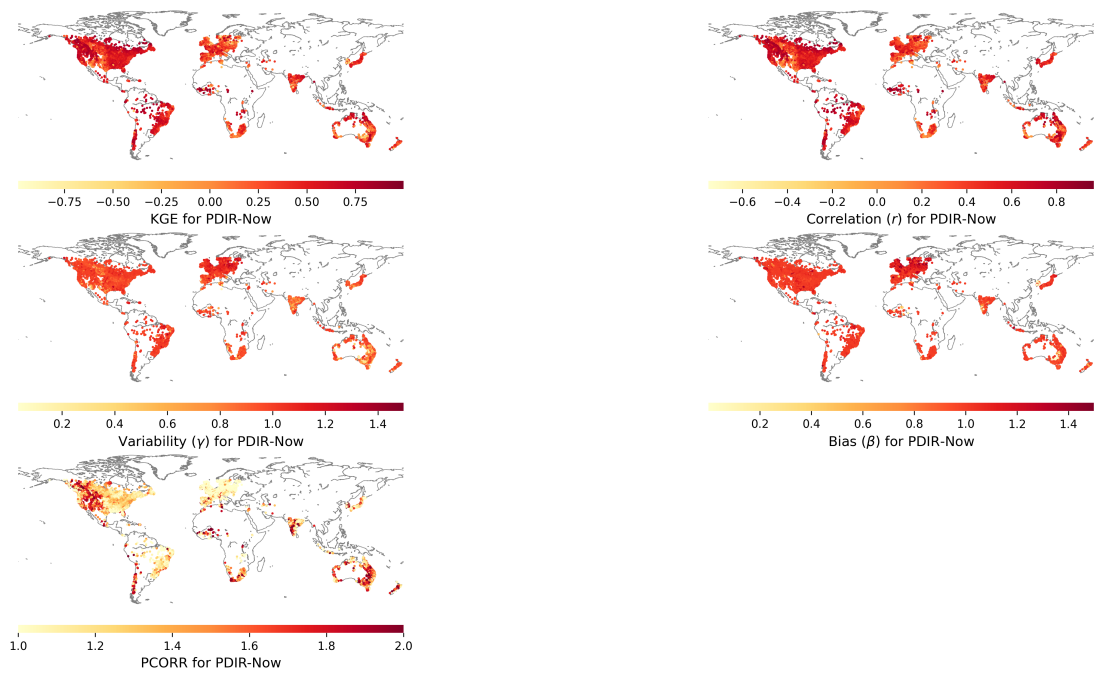


Figure S22: Calibration performance (KGE, correlation, variability, and bias) and PCORR values for PDIR-Now.

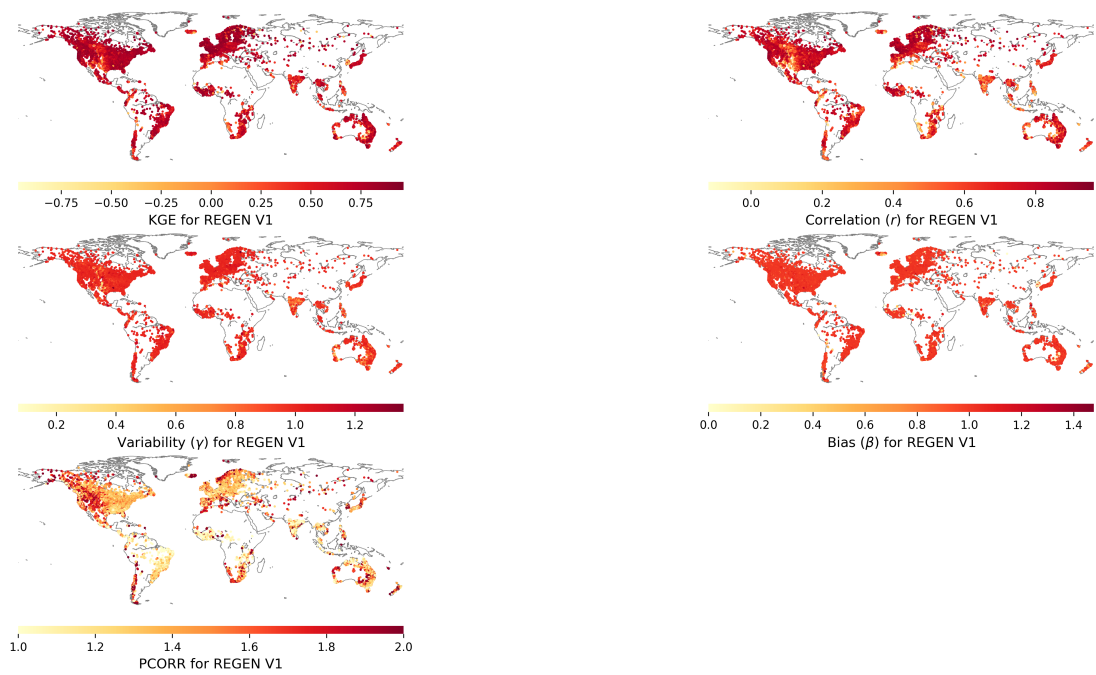


Figure S23: Calibration performance (KGE, correlation, variability, and bias) and PCORR values achieved for GPM+SM2RAIN.

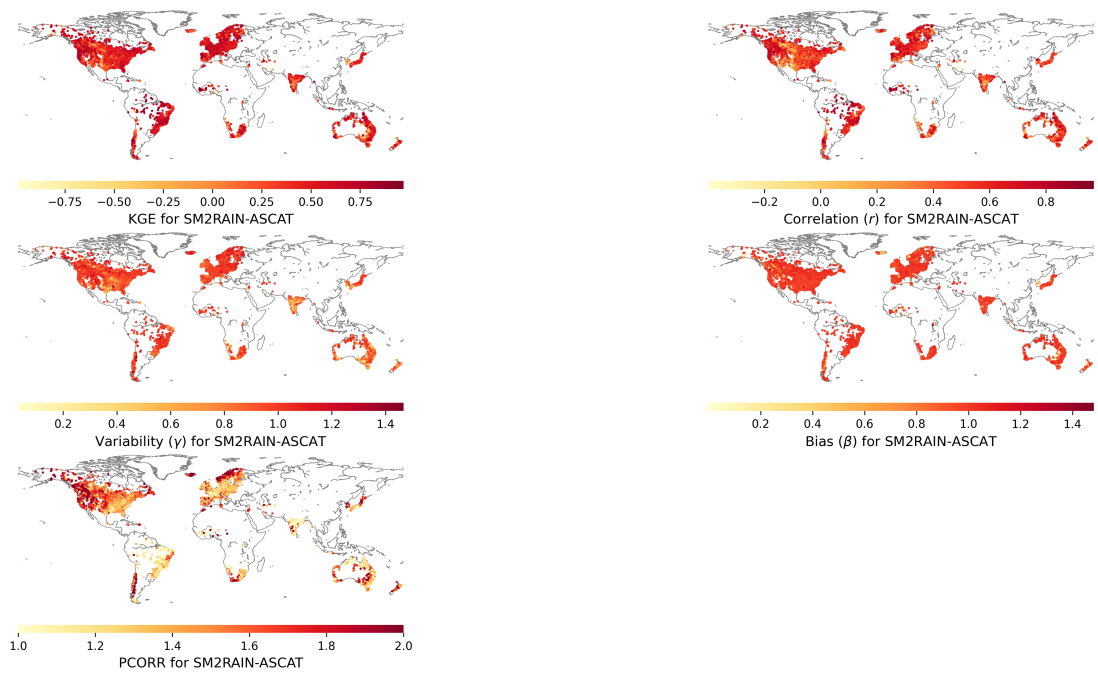


Figure S24: Calibration performance (KGE, correlation, variability, and bias) and PCORR values for SM2RAIN-ASCAT.

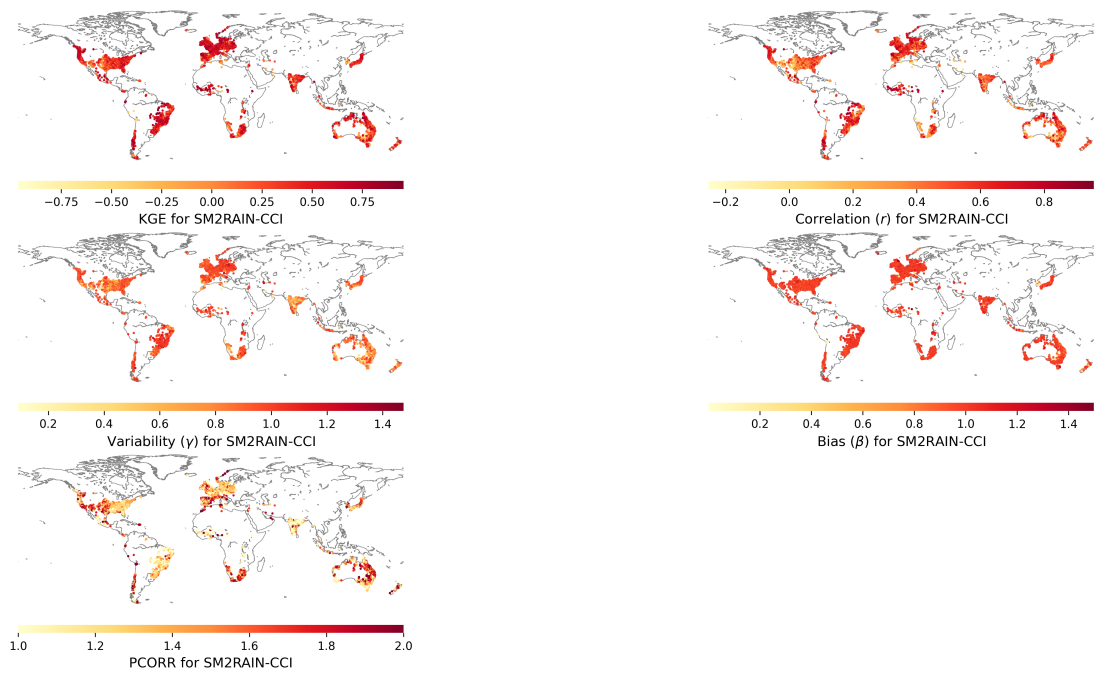


Figure S25: Calibration performance (KGE, correlation, variability, and bias) and PCORR values achieved for SM2RAIN-CCI.

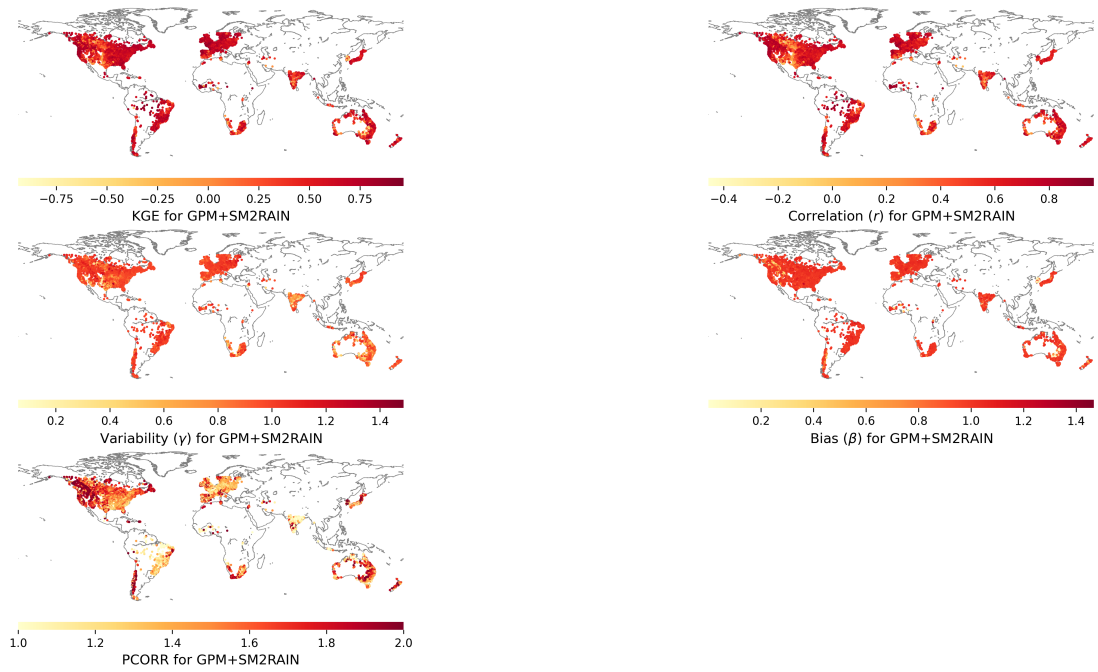


Figure S26: Calibration performance (KGE, correlation, variability, and bias) and PCORR values for GPM+SM2RAIN.

### S3 Performance Variation Across Streamflow Data Sources

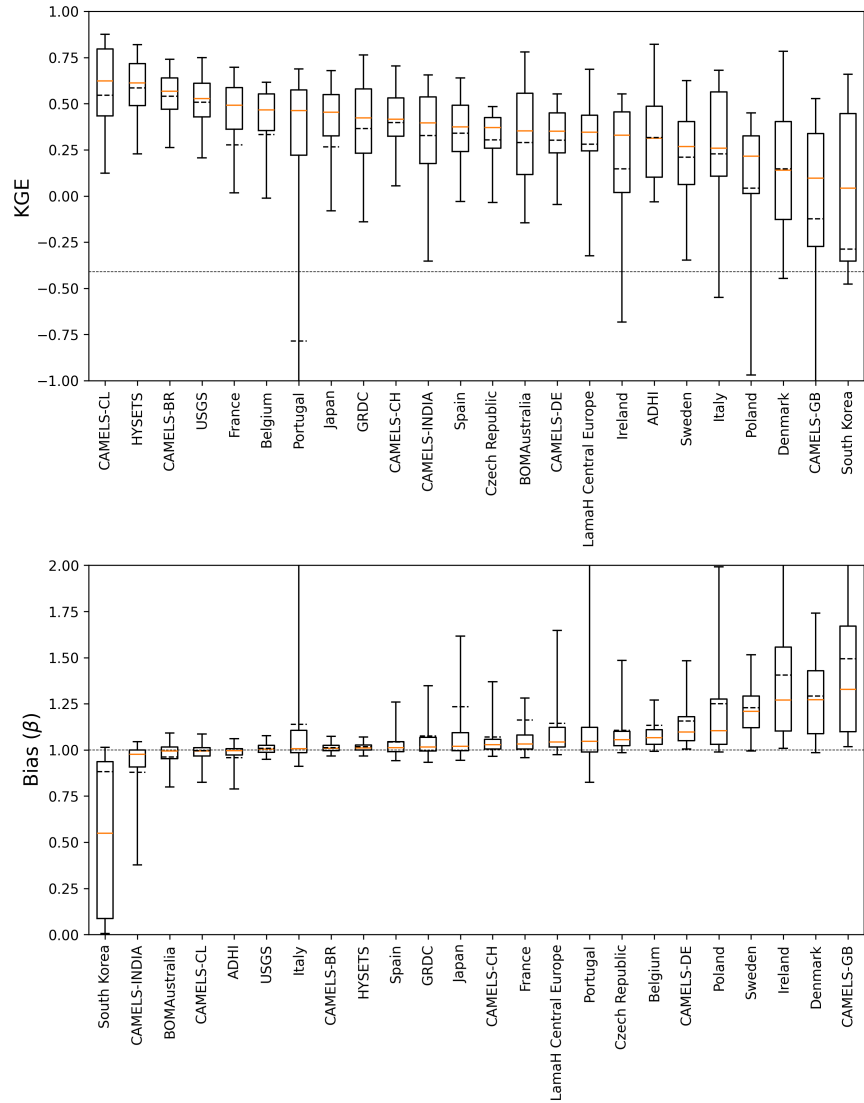


Figure S27: Distribution of calibration KGE and bias for different streamflow data sources for PDIR-Now.

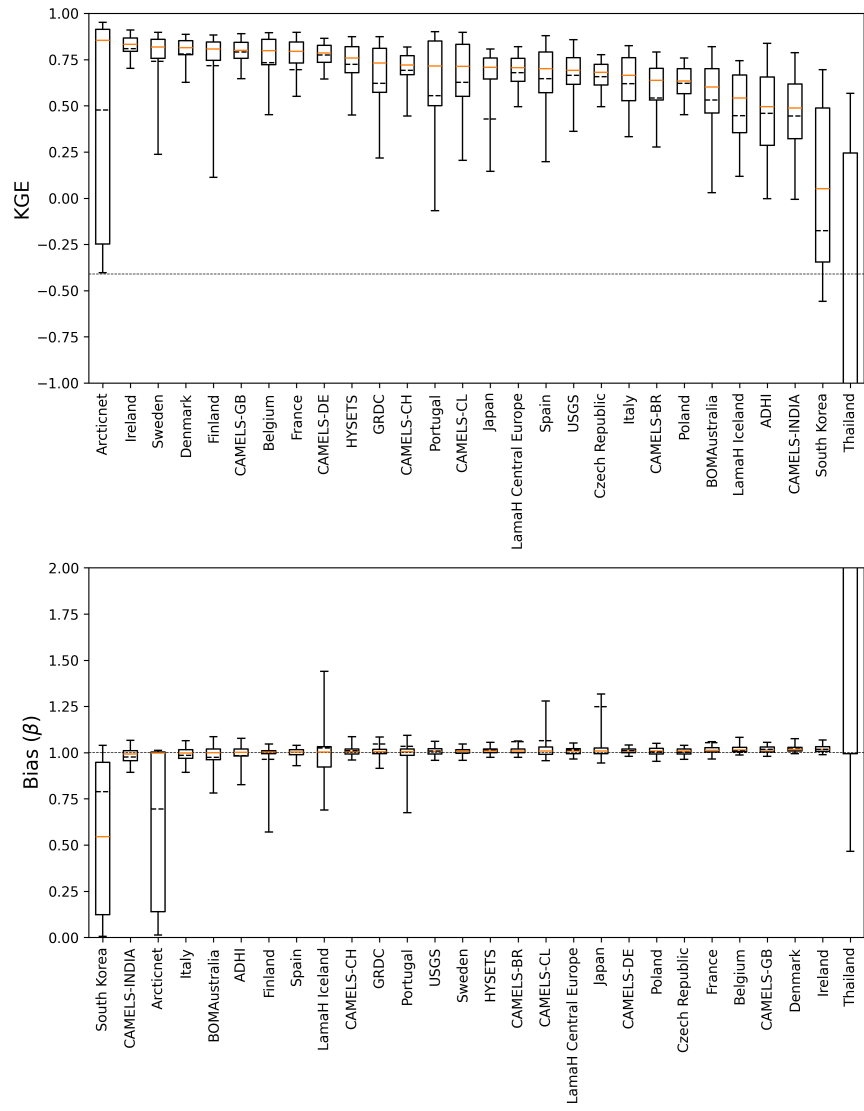


Figure S28: Distribution of calibration KGE and bias for different streamflow data sources for JRA-3Q.

## S4 Impact of Rain Gauge Density on Model Performance

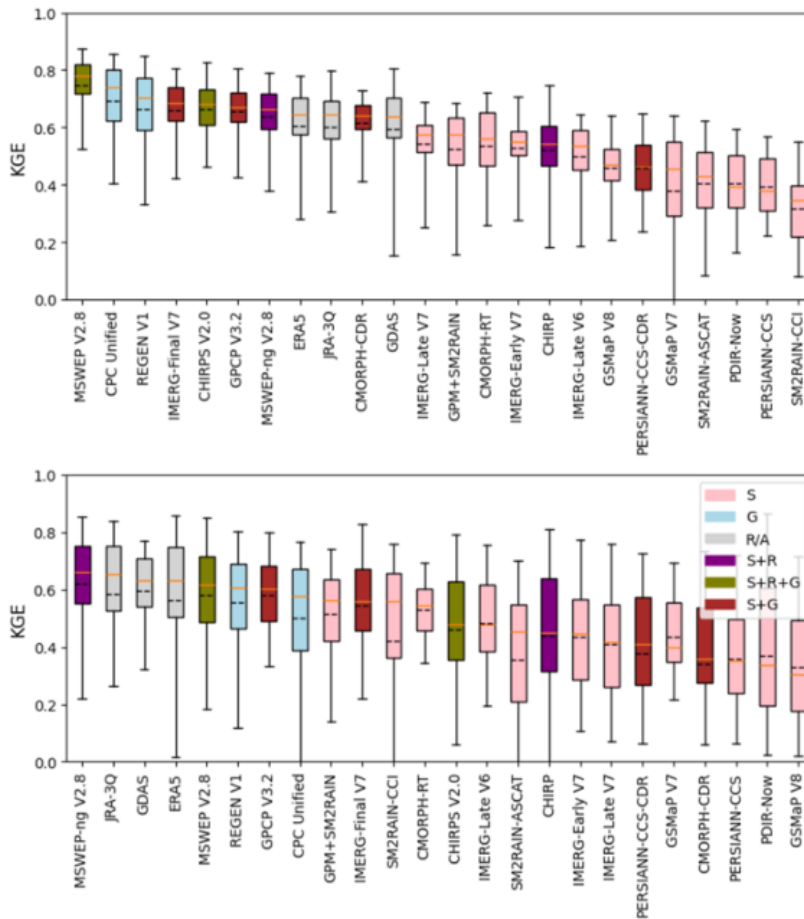


Figure S29: Comparison of  $P$  dataset performance for 100 catchments with highest rain gauge densities (top) vs 100 catchments with lowest rain gauge densities (bottom)

## S5 Scenario Analysis of Calibration Strategies

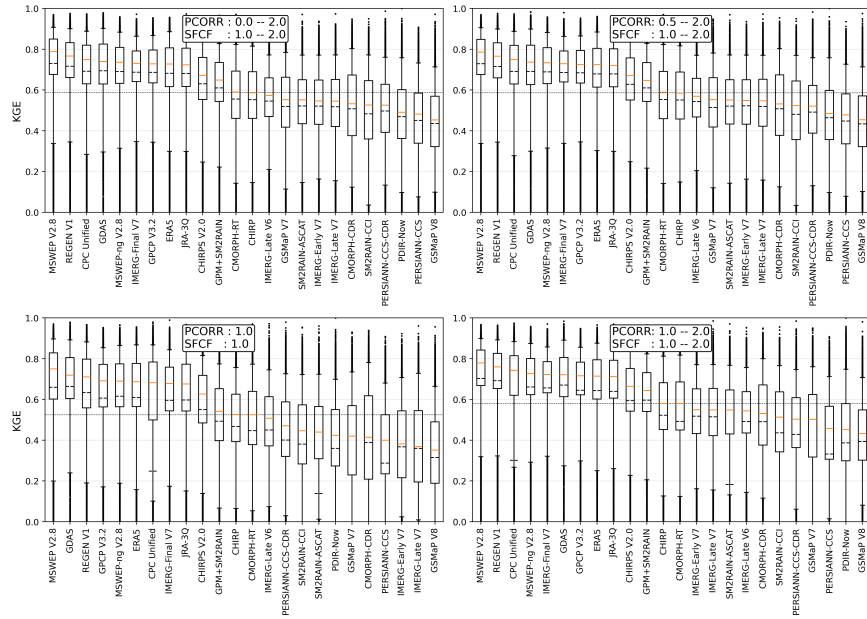


Figure S30: Kling-Gupta Efficiency values for  $P$  datasets in different scenarios of PCORR and SFCF calibration.

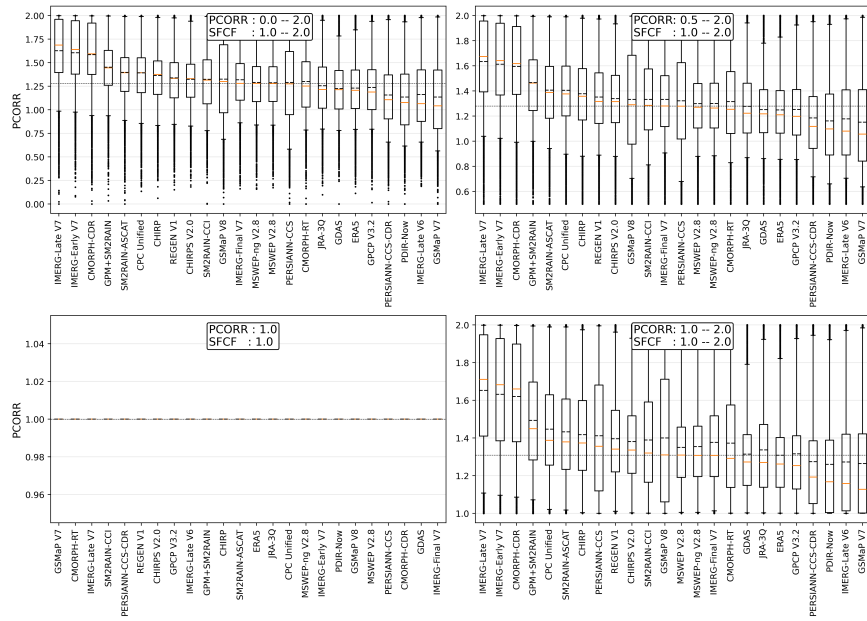


Figure S31: Comparison of distribution of calibrated PCORR values from four calibration scenarios.

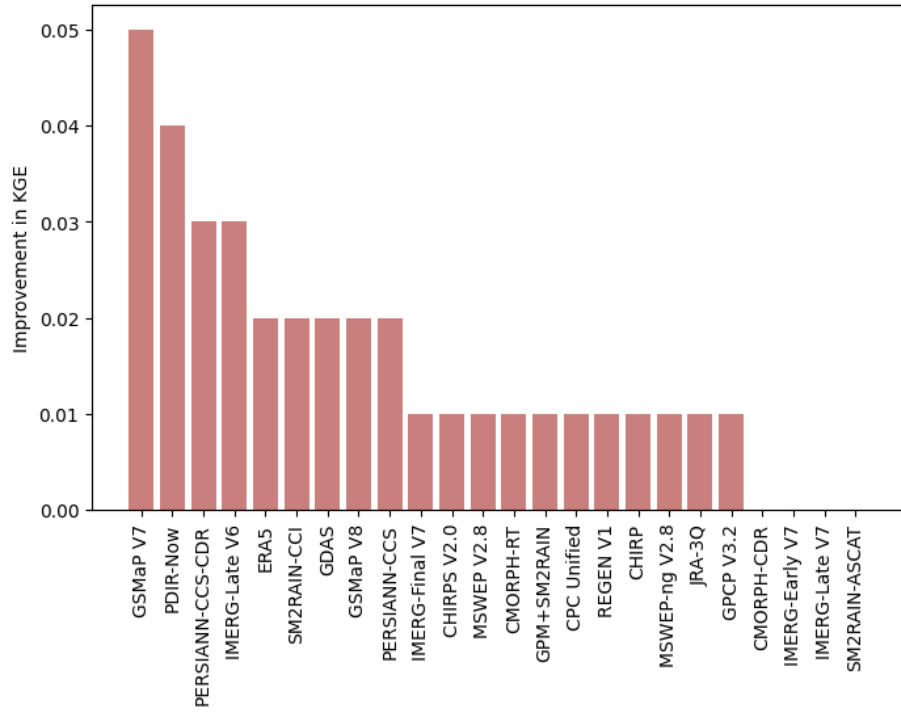


Figure S32: Improvement in KGE values for different P datasets by increasing the range of PCORR from 1.0-2.0 to 0.0 to 2.0 during calibration.

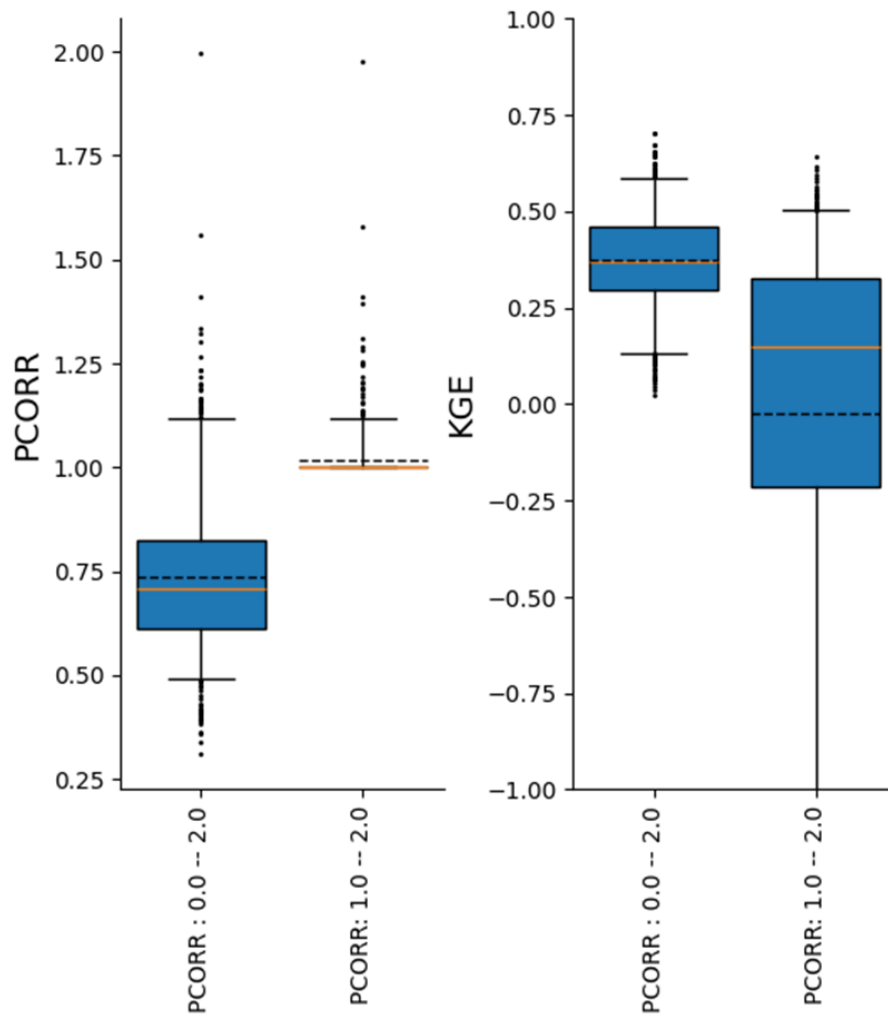


Figure S33: Comparison of calibrated PCORR and corresponding KGE values from 531 catchments from CAMELS-GB using PDIR-Now P dataset.

## S6 Differences in Mean Annual Precipitation

This section includes 24 maps displaying difference between the mean annual  $P$  of each product and the multi-product mean.

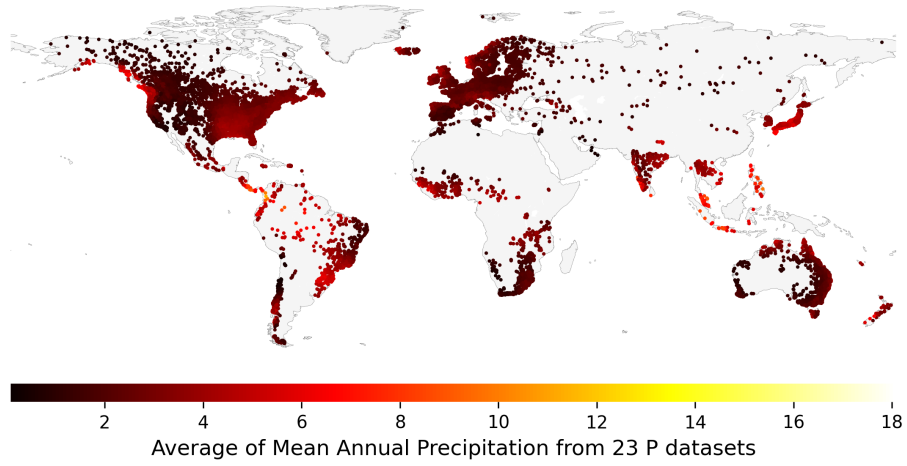


Figure S34: Average of the mean annual precipitation from 24 datasets.

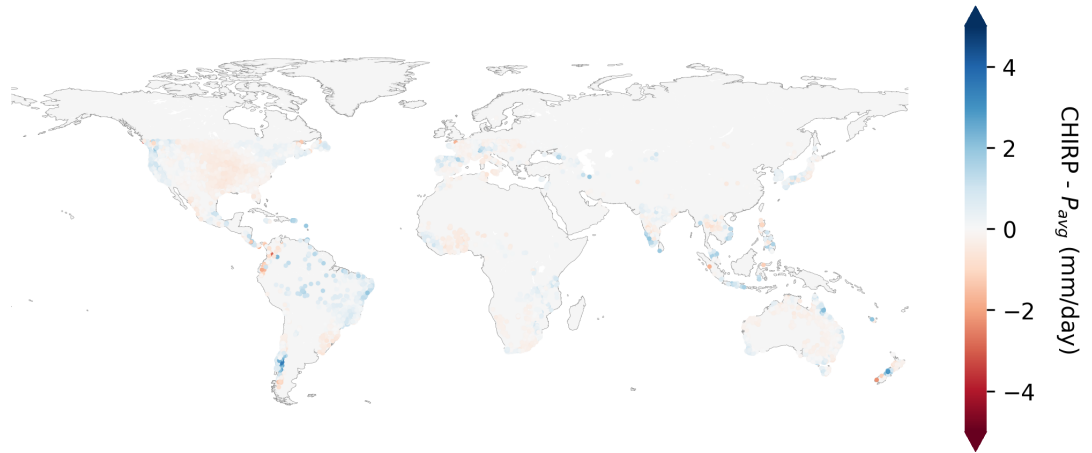


Figure S35: Difference between mean annual precipitation of CHIRP and average of mean annual precipitation of all datasets ( $P_{avg}$ ).

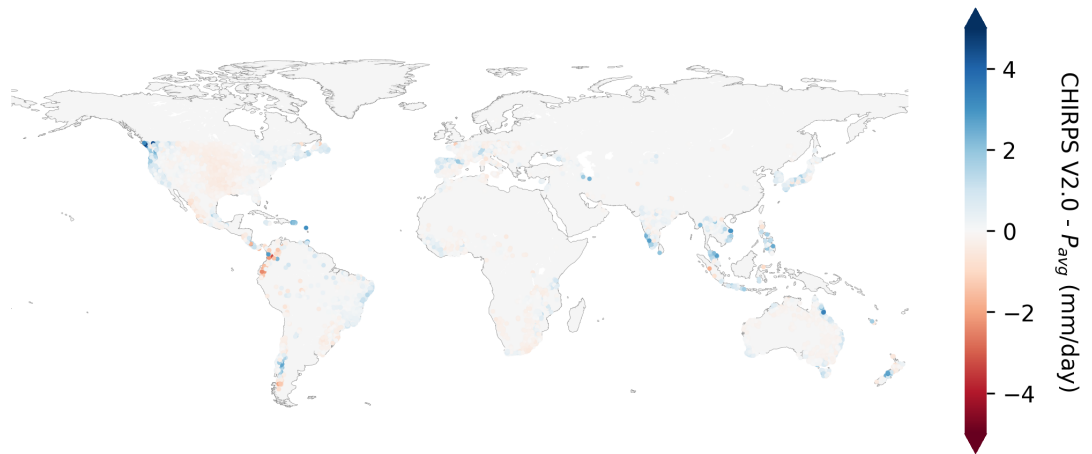


Figure S36: Difference between mean annual precipitation of CHIRPS V2.0 and average of mean annual precipitation of all datasets ( $P_{avg}$ ).

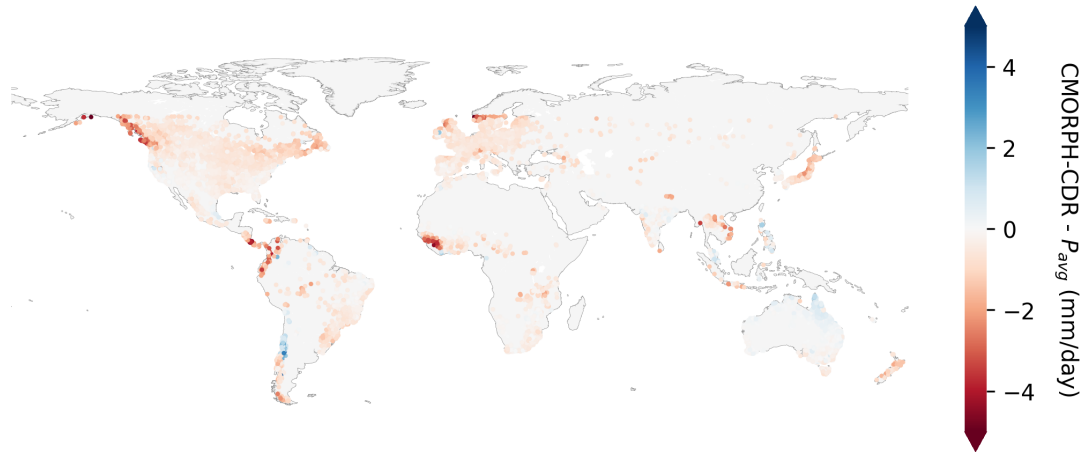


Figure S37: Difference between mean annual precipitation of CMORPH-CDR Unified and average of mean annual precipitation of all datasets ( $P_{avg}$ ).

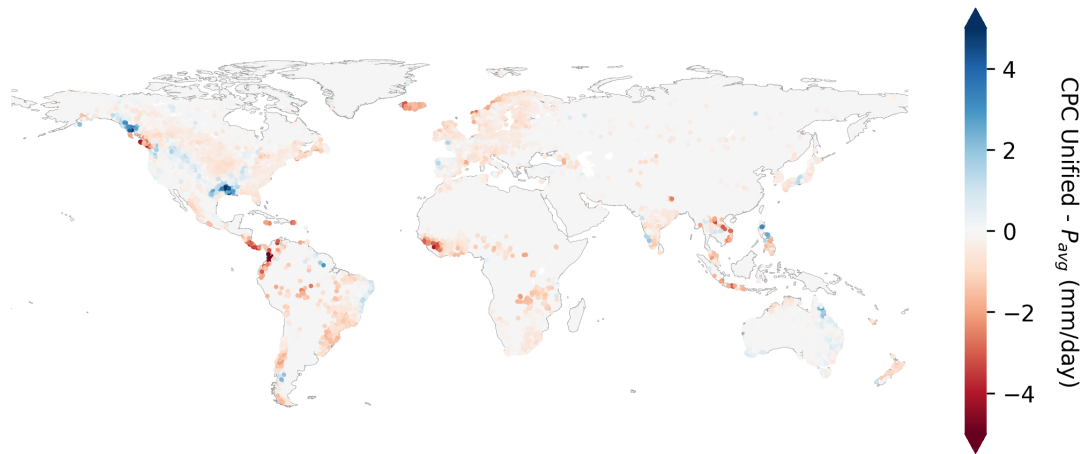


Figure S38: Difference between mean annual precipitation of CPC Unified and average of mean annual precipitation of all datasets ( $P_{avg}$ ).

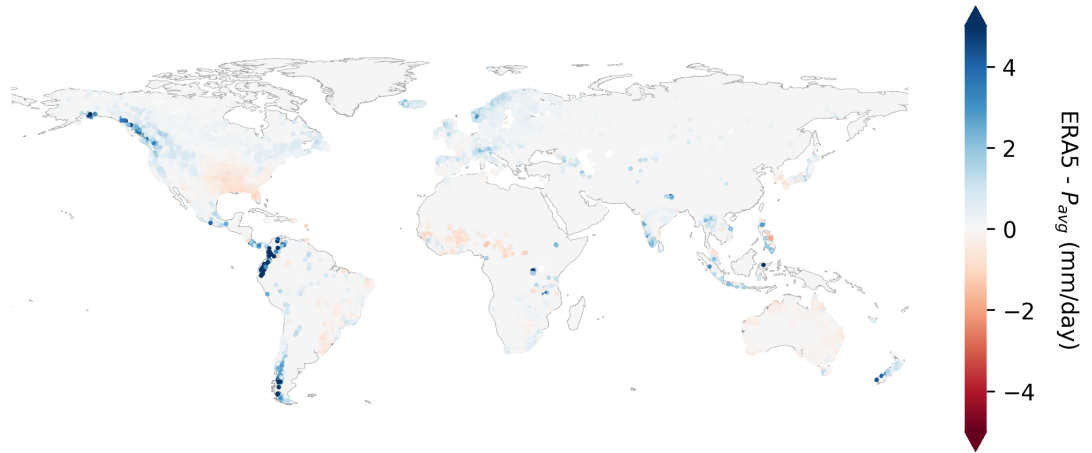


Figure S39: Difference between mean annual precipitation of ERA5 and average of mean annual precipitation of all datasets ( $P_{avg}$ ).

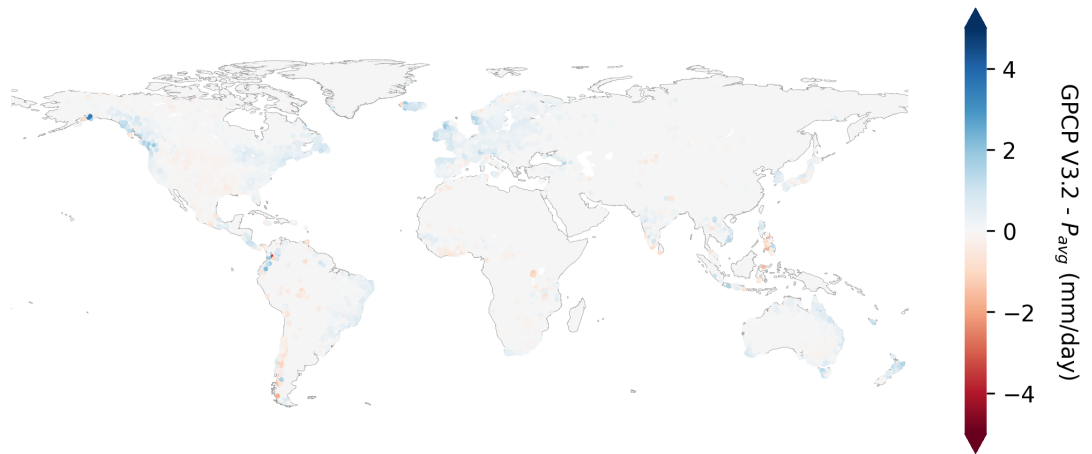


Figure S40: Difference between mean annual precipitation of GPCP V3.2 and average of mean annual precipitation of all datasets ( $P_{avg}$ ).

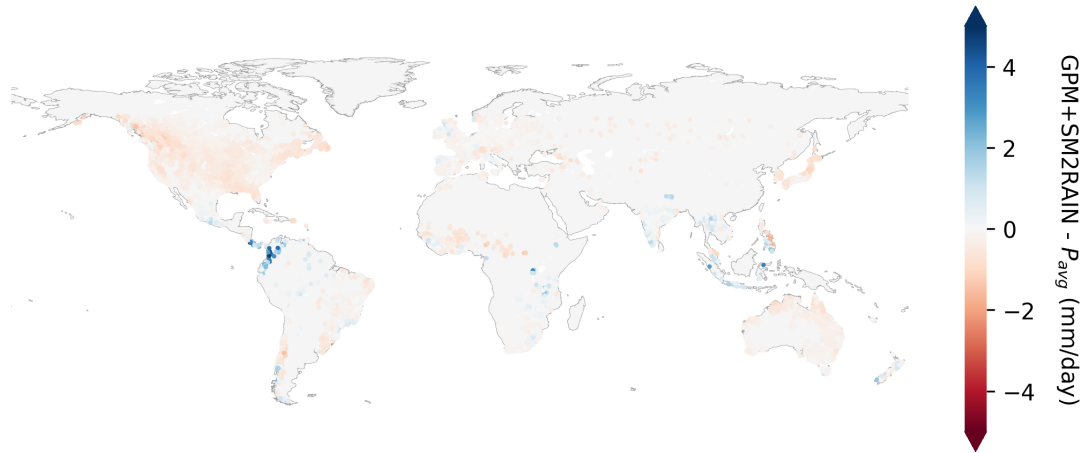


Figure S41: Difference between mean annual precipitation of GPM+SM2RAIN and average of mean annual precipitation of all datasets ( $P_{avg}$ ).

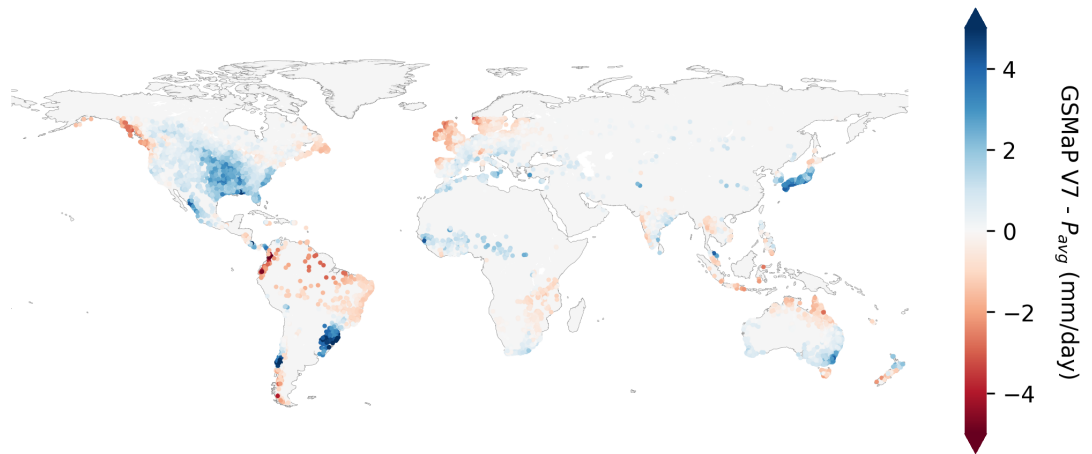


Figure S42: Difference between mean annual precipitation of GSMaP V7 and average of mean annual precipitation of all datasets ( $P_{avg}$ ).

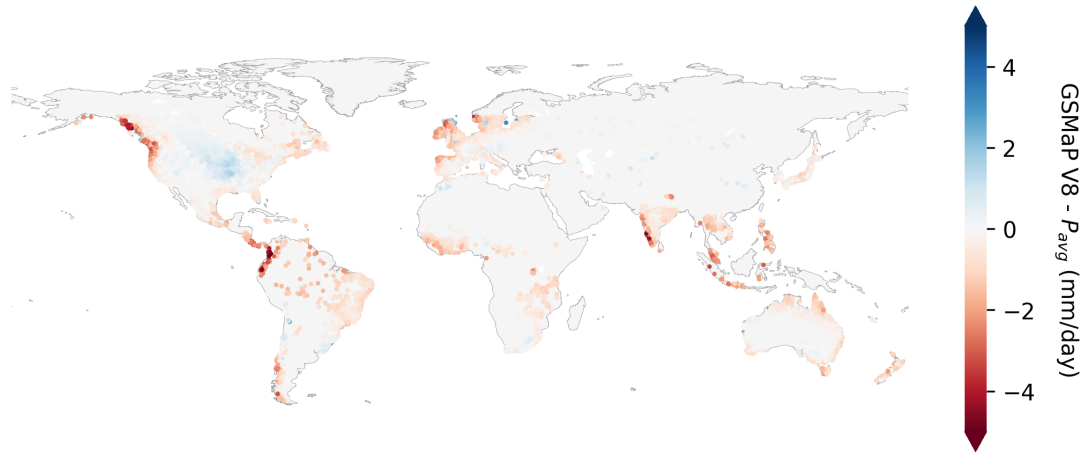


Figure S43: Difference between mean annual precipitation of GSMaP V8 and average of mean annual precipitation of all datasets ( $P_{avg}$ ).

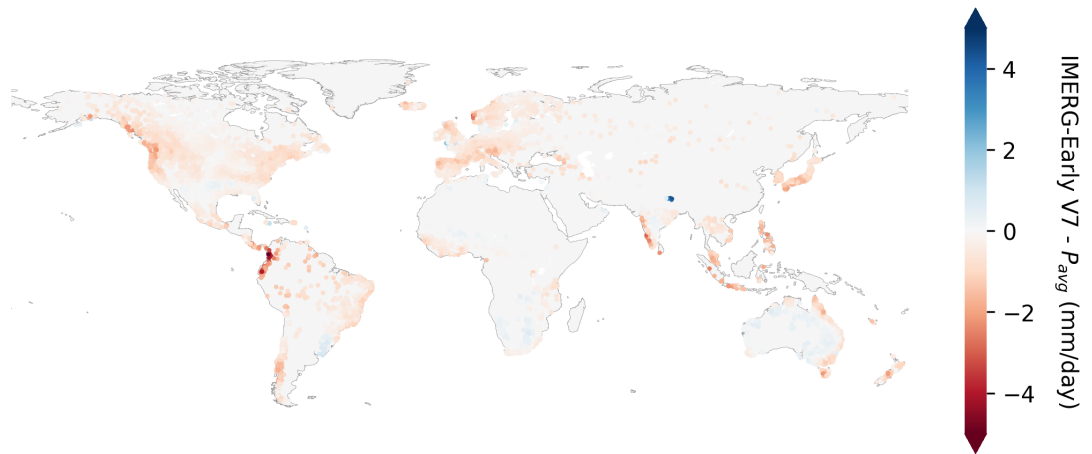


Figure S44: Difference between mean annual precipitation of IMERG-Early V7 and average of mean annual precipitation of all datasets ( $P_{avg}$ ).

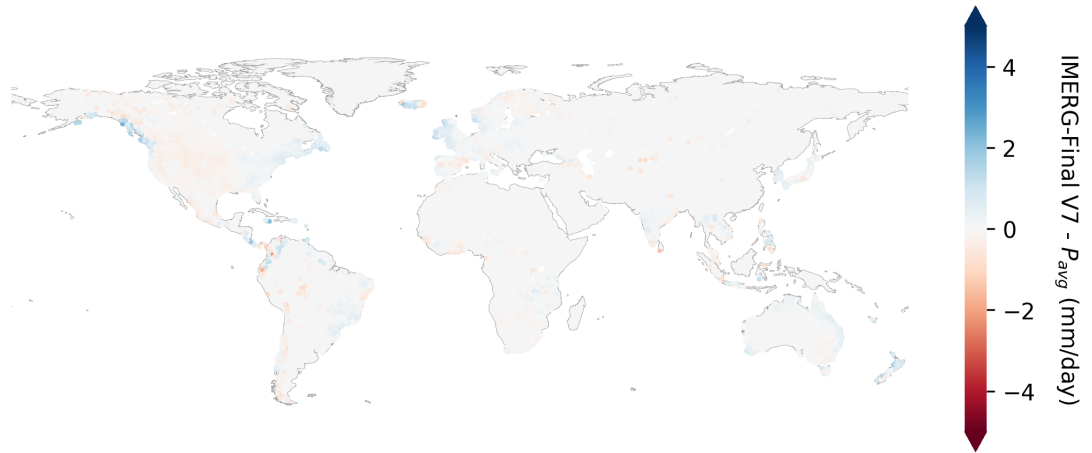


Figure S45: Difference between mean annual precipitation of IMERG-Final V7 and average of mean annual precipitation of all datasets ( $P_{avg}$ ).

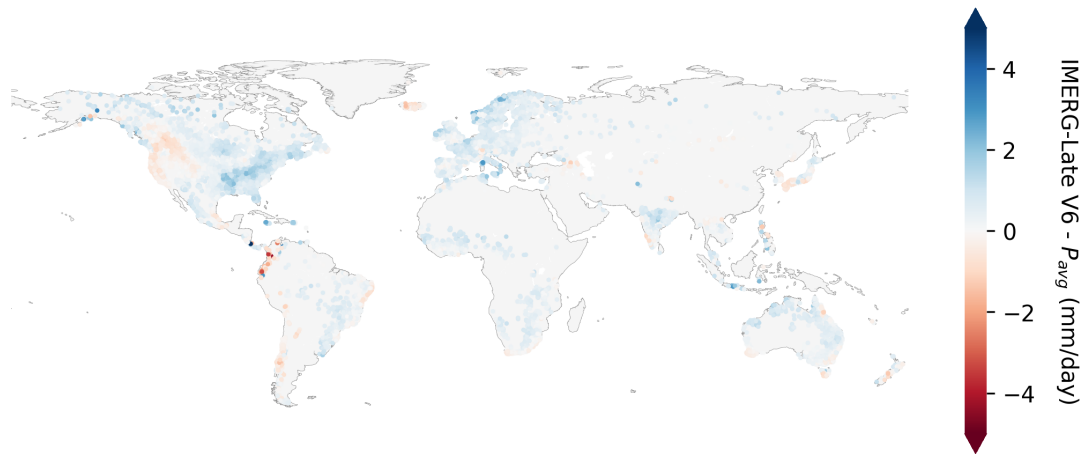


Figure S46: Difference between mean annual precipitation of IMERG-Late V6 and average of mean annual precipitation of all datasets ( $P_{avg}$ ).

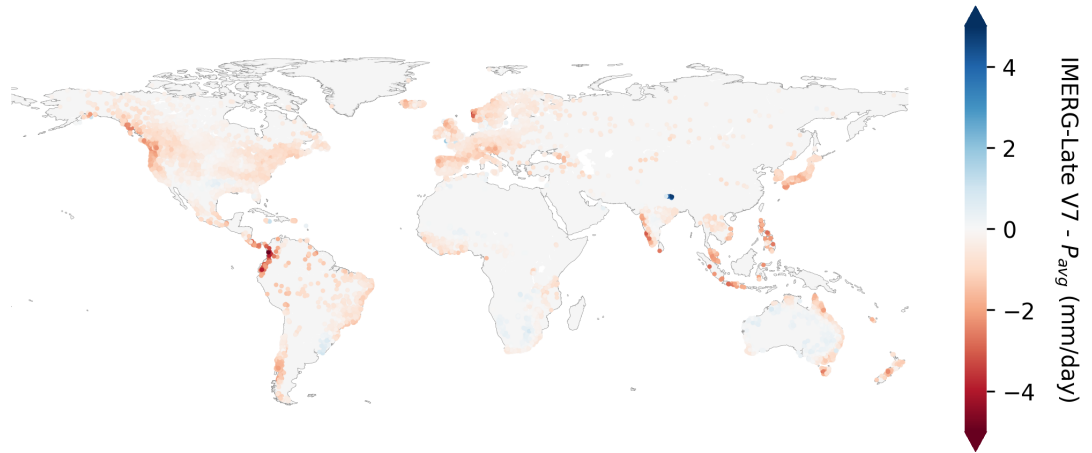


Figure S47: Difference between mean annual precipitation of IMERG-Late V7 and average of mean annual precipitation of all datasets ( $P_{avg}$ ).

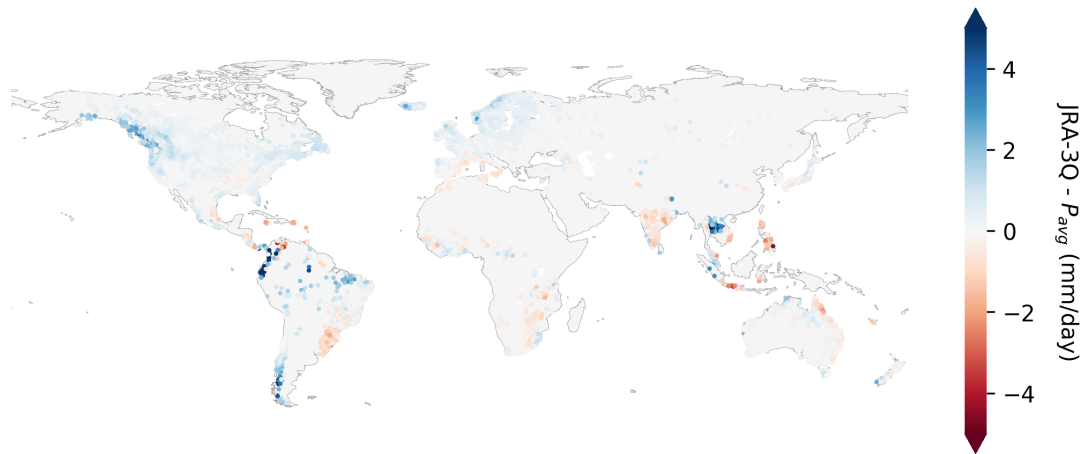


Figure S48: Difference between mean annual precipitation of JRA-3Q and average of mean annual precipitation of all datasets ( $P_{avg}$ ).

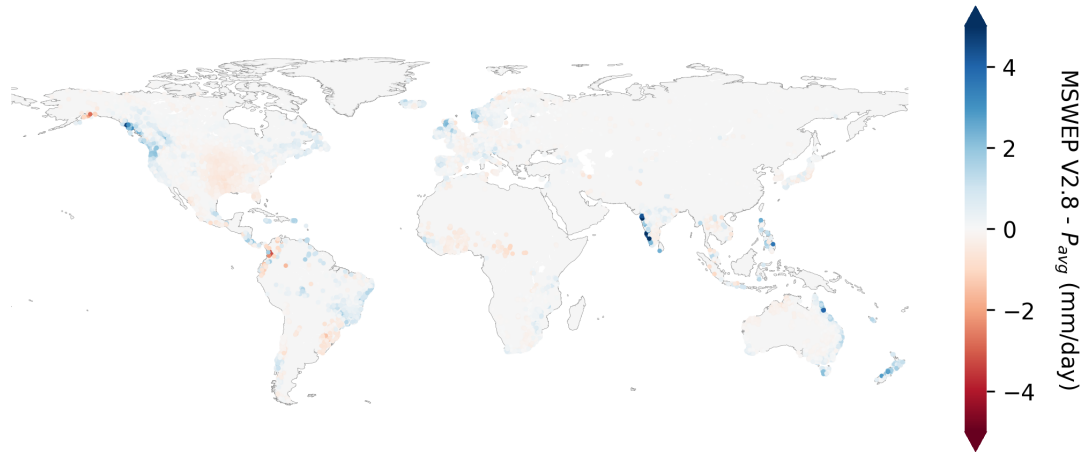


Figure S49: Difference between mean annual precipitation of MSWEP V2.8 and average of mean annual precipitation of all datasets ( $P_{avg}$ ).

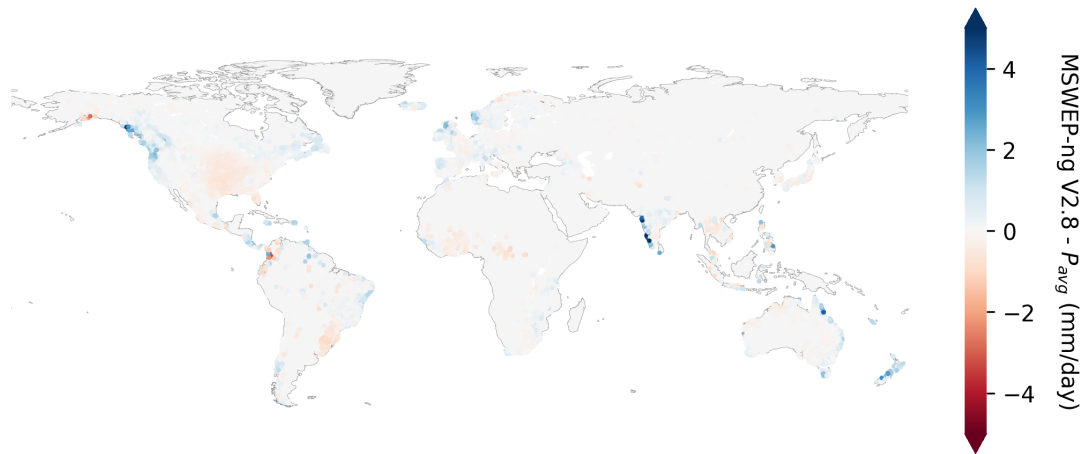


Figure S50: Difference between mean annual precipitation of MSWEP-ng V2.8 and average of mean annual precipitation of all datasets ( $P_{avg}$ ).

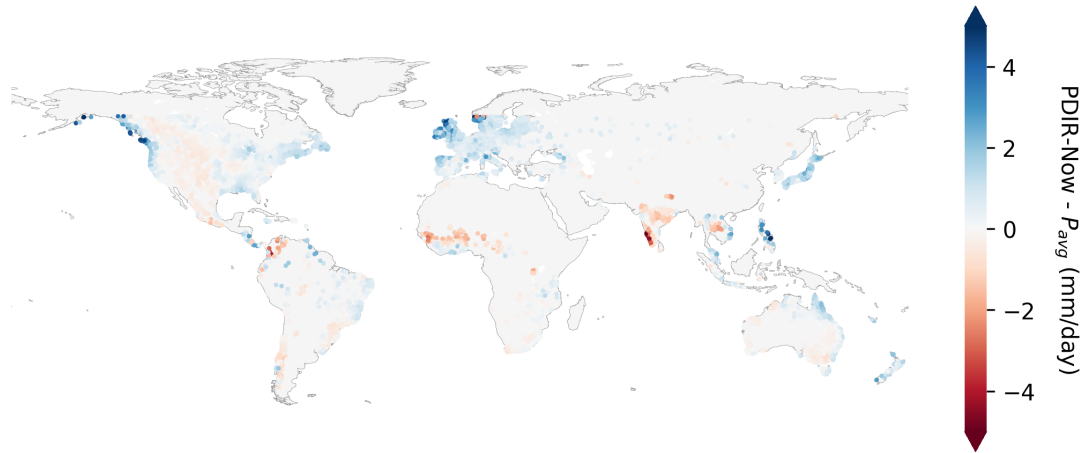


Figure S51: Difference between mean annual precipitation of PDIR-Now and average of mean annual precipitation of all datasets ( $P_{avg}$ ).

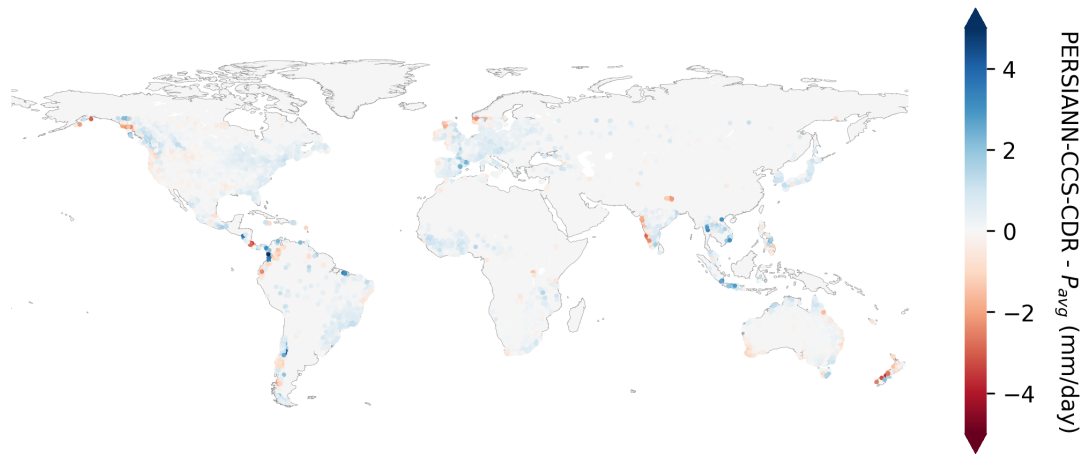


Figure S52: Difference between mean annual precipitation of PERSIANN-CCS-CDR and average of mean annual precipitation of all datasets ( $P_{avg}$ ).

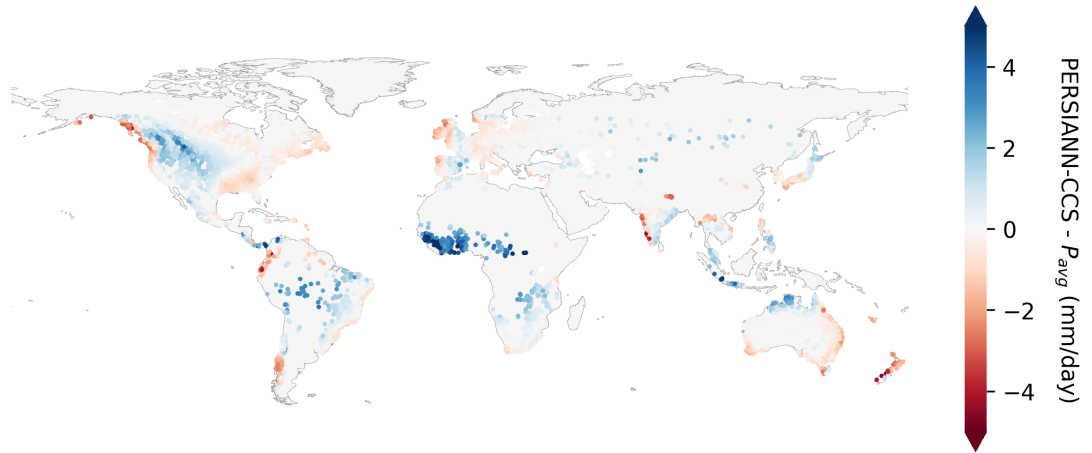


Figure S53: Difference between mean annual precipitation of PERSIANN-CCS and average of mean annual precipitation of all datasets ( $P_{avg}$ ).

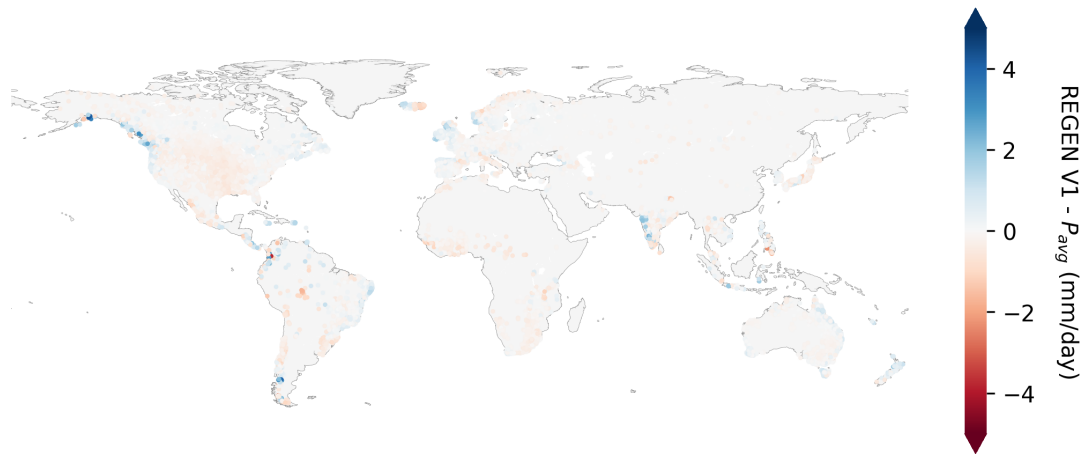


Figure S54: Difference between mean annual precipitation of PERSIANN-CCS and average of mean annual precipitation of all datasets ( $P_{avg}$ ).

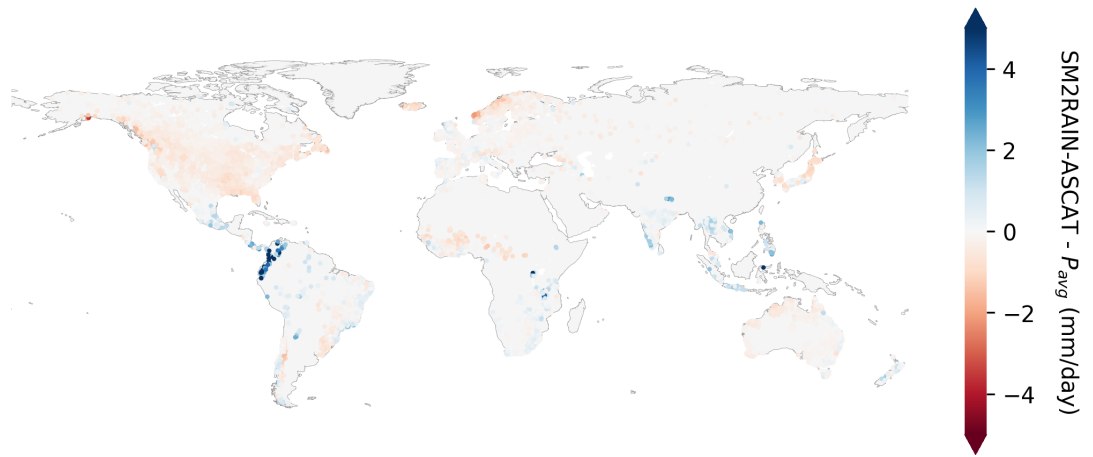


Figure S55: Difference between mean annual precipitation of SM2RAIN-ASCAT and average of mean annual precipitation of all datasets ( $P_{avg}$ ).

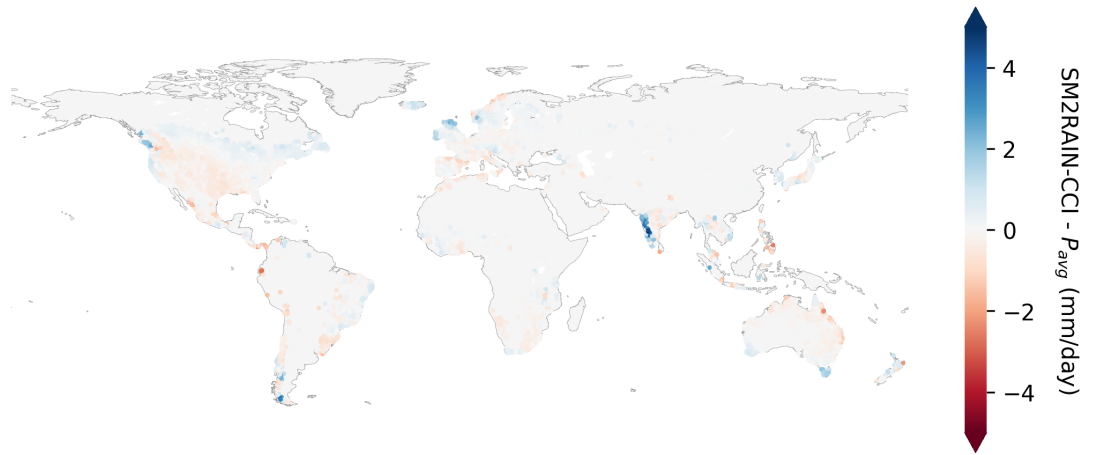


Figure S56: Difference between mean annual precipitation of SM2RAIN-CCI and average of mean annual precipitation of all datasets ( $P_{avg}$ ).

## S7 Performance Variation with Altitude

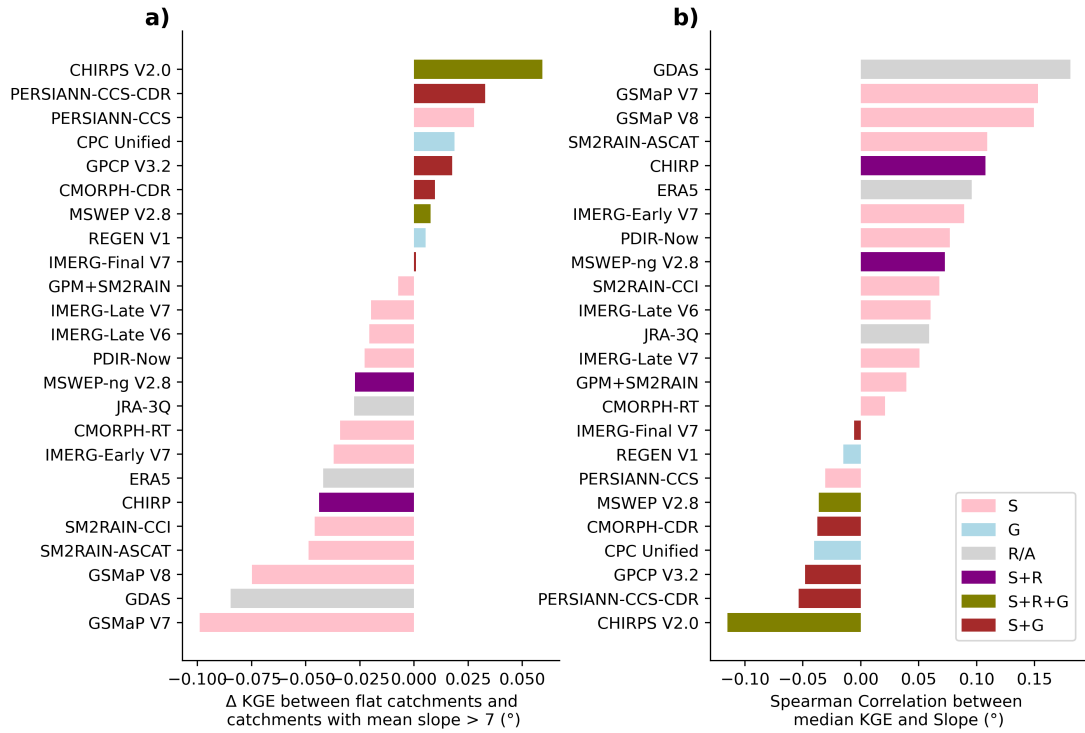


Figure S57: Variation in HBV performance (KGE) with increase in slope.